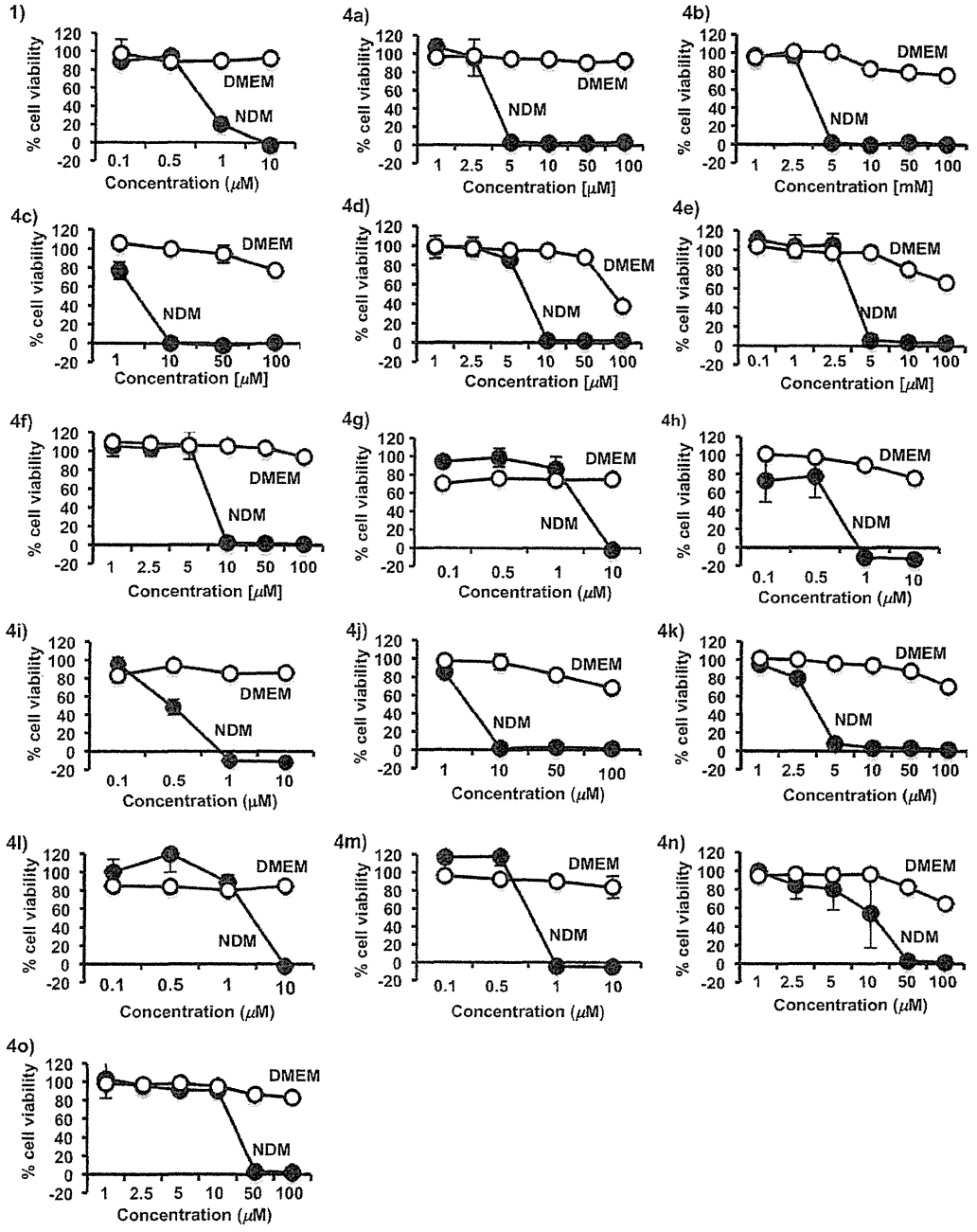

Fig. 2. Effects of (−)-arctigenin derivatives on cell survival in the PANC-1 cell line under nutrient-deprived conditions. Cells were seeded at a density of 2×10^4 per well in 96-well plates and incubated in fresh complete medium for 24 h. The cells were then washed with PBS and the medium was changed to nutrient-deprived medium (NDM, ●) or normal DMEM (○) together containing graded concentrations of (−)-arctigenin derivatives. Points, mean from triplicate experiments. The cell number at the start of the starvation was considered to be 100%. The cell count was measured by the WST-8 cell counting kit method, as described in experimental. The numbers **1** and **4a–o** mean the data of (−)-arctigenin (**1**) and (−)-arctigenin derivatives **4a–o**, respectively.

130.59, 144.52, 147.69, 178.54; IR (neat): 1456 (C=C), 1769 (C=O) cm^{-1}; MS (EI) *m/z* 400 (M^+); HRMS (EI): calcd for $C_{23}H_{28}O_6$: 400.1886 (M^+), found: 400.1893; $[\alpha]_D^{26}$ −15.7 (*c* 1.45, $CHCl_3$).

*4.1.2.4. (3R,4R)-4-(3,4-Dimethoxybenzyl)-3-(4-hydroxy-3-i-propoxybenzyl)dihydrofuran-2-one (**4c**).* By the procedure similar to synthesis of **4a**, (−)-arctigenin derivative **4c** was prepared from **3** and *i*-PrI (18% in 2 steps) as a pale yellow oil: ^1H NMR (300 MHz, $CDCl_3$) δ: 1.31–1.35 (6H, m), 1.59 (1H, br), 2.41–2.68 (4H, m), 2.80–3.00 (2H, m), 3.80–3.88 (7H, m), 4.07–4.12 (1H, m), 4.49–4.57 (1H, m), 6.48–6.84 (6H, m); ^{13}C NMR (75 MHz, $CDCl_3$) δ: 22.02, 34.39, 3.12, 41.45, 46.65, 55.81, 71.19, 111.25, 111.68, 113.41, 114.18, 115.49, 120.61, 122.09, 129.26, 130.43, 144.70, 145.48, 146.59, 147.84, 149.02, 178.72; IR (neat): 1716 (C=O), 3629 (OH) cm^{-1}; MS (EI) *m/z* 400 (M^+); HRMS (EI): calcd for $C_{23}H_{28}O_6$: 400.1886 (M^+), found: 400.1926; $[\alpha]_D^{24}$ −37.7 (*c* 0.41, $CHCl_3$).

*4.1.2.5. (3R,4R)-4-(3,4-Dimethoxybenzyl)-3-(4-hydroxy-3-butyloxybenzyl)dihydrofuran-2-one (**4d**).* By the procedure similar to synthesis of **4a**, (−)-arctigenin derivative **4d** was prepared from **3**

Table 1
Preferential cytotoxicity of (−)-arctigenin (**1**) and series of new (−)-arctigenin derivatives **4a**–**4o** against human pancreatic cancer PANC-1 cells in nutrient-deprived medium (NDM).

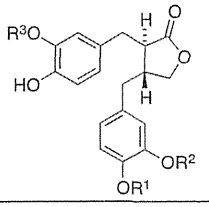

Compound	R^1	R^2	R^3	PC_{50} (μM)	Compound	R^1	R^2	R^3	PC_{50} (μM)
1 (arctigenin)	Me	Me	Me	0.80	**4h**	Me	Et	Et	0.66
4a	Me	Me	Et	3.74	**4i**	Et	Me	Me	0.49
4b	Me	Me	*n*-Pr	3.74	**4j**	Et	Me	Et	4.77
4c	Me	Me	*i*-Pr	4.16	**4k**	Me	Et	*n*-Pr	3.54
4d	Me	Me	*n*-Bu	7.14	**4l**	Et	Et	Me	4.85
4e	Me	Me	*n*-Hex	3.89	**4m**	Et	Et	Et	0.78
4f	Me	Me	$HO(CH_2)_2$	7.70	**4n**	Me	*n*-Pr	*n*-Pr	13.6
4g	Me	Et	Me	4.71	**4o**	Et	*n*-Pr	*n*-Pr	28.6

and *n*-BuBr (25% in 2 steps) as a colorless oil: ^{1}H NMR (300 MHz, $CDCl_3$) δ: 0.98 (3H, t, J = 7.1 Hz), 1.48 (2H, dd, J = 15.1, 7.1 Hz), 1.74–1.83 (2H, m), 2.41–2.66 (4H, m), 2.80–3.02 (2H, m), 3.82 (3H, s), 3.83 (3H, s), 3.85 (1H, m), 3.94–4.03 (2H, m), 4.08–4.14 (1H, m), 5.59 (1H, m), 6.50–6.84 (6H, m); ^{13}C NMR (75 MHz, $CDCl_3$) δ: 13.97, 19.32, 31.31, 55.82, 55.92, 68.60, 68.65, 71.21, 71.27, 111.19, 111.67, 112.32, 113.92, 120.46, 129.29, 130.34, 130.46, 144.52, 144.71, 145.59, 145.96, 147.69, 148.92, 178.53; IR (neat): 1515 (C=C), 1769 (C=O), 3446 (OH) cm^{-1}; MS (EI) *m/z* 414 (M^+); HRMS (EI): calcd for $C_{24}H_{30}O_6$: 414.2042 (M^+), found: 414.2000; $[\alpha]_D^{26}$ −20.2 (*c* 1.15, $CHCl_3$).

*4.1.2.6. (3R,4R)-4-(3,4-Dimethoxybenzyl)-3-(3-hexyloxy-4-hydroxybenzyl)dihydrofuran-2-one (**4e**).* By the procedure similar to synthesis of **4a**, (−)-arctigenin derivative **4e** was prepared from **3** and 1-bromohexane (35% in 2 steps) as a pale yellow oil: ^{1}H NMR (300 MHz, $CDCl_3$) δ: 0.90 (3H, t, J = 6.4 Hz), 1.25–1.27 (2H, m), 1.33–1.35 (4H, m), 1.45 (2H, m), 1.75–2.66 (4H, m), 2.81–3.01 (2H, m), 3.82 (3H, s), 3.85 (3H, s), 3.84–3.89 (1H, m), 3.94–4.02 (2H, m), 4.09–4.14 (1H, m), 5.56–5.61 (1H, m), 6.47–6.84 (6H, m); ^{13}C NMR (75 MHz, $CDCl_3$) δ: 14.11, 22.67, 25.78, 29.25, 31.62, 34.56, 38.22, 40.02, 46.65, 55.82, 68.92, 71.21, 111.19, 111.67, 112.32, 113.92, 115.25, 120.56, 121.83, 129.29, 130.43, 130.34, 144.52, 147.67, 148.92, 178.53; IR (neat): 1457 (C=C), 1764 (C=O), 3689 (OH) cm^{-1}; MS (EI) *m/z* 442 (M^+); HRMS (EI): calcd for $C_{26}H_{34}O_6$: 442.2355 (M^+), found: 442.2336; $[\alpha]_D^{26}$ −10.1 (*c* 0.65, $CHCl_3$).

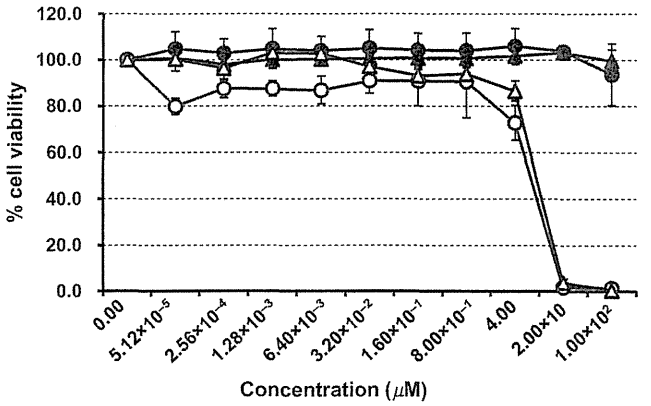

Fig. 3. Effect of triethoxy derivative **4m** and (−)-arctigenin (**1**) on cell survival in the CAPAN-1 cell line under glucose-deprived conditions. ●, (−)-arctigenin (**1**) in normal DMEM; ▲, triethoxy derivative **4m** in normal DMEM; ○, (−)-arctigenin (**1**) in glucose-deprived medium; △, triethoxy derivative **4m** in glucose-deprived medium.

*4.1.2.7. (3R,4R)-4-(3,4-Dimethoxybenzyl)-3-[4-hydroxy-3-(2-hydroxyethoxy)benzyl]dihydrofuran-2-one (**4f**).* By the procedure similar to synthesis of **4a**, (−)-arctigenin derivative **4f** was prepared from **3** and 2-benzyloxyethanol (20% in 2 steps) as a colorless oil: ^{1}H NMR (300 MHz, $CDCl_3$) δ: 2.42–2.59 (4H, m), 2.78–2.94 (2H, m), 3.76 (3H, s), 3.83 (3H, s), 3.73–3.80 (1H, m), 3.86–4.07 (6H, m), 4.13–4.16 (1H, m), 6.40–6.75 (4H, m), 6.81 (1H, d, J = 8.0 Hz); ^{13}C NMR (75 MHz, $CDCl_3$) δ: 28.24, 38.22, 40.69, 46.53, 55.72, 55.97, 61.08, 69.82, 71.45, 111.30, 111.56, 113.00, 115.02, 120.67, 122.55, 129.00, 130.44, 145.02, 146.10, 147.38, 148.72, 178.83; IR (neat): 1517 (C=C), 1765 (C=O), 3420 (OH) cm^{-1}; MS (EI) *m/z* 402 (M^+); HRMS (EI): calcd for $C_{23}H_{28}O_6$: 402.1679 (M^+), found: 402.1671; $[\alpha]_D^{26}$ −19.7 (*c* 1.10, $CHCl_3$).

*4.1.3. Synthesis of (−)-arctigenin derivatives **4g**–**4o***

*4.1.3.1. (4-Benzyloxy-3-methoxymethoxyphenyl)methanol (**7**).* To a stirred solution of 4-benzyloxy-3-methoxymethoxybenzaldehyde (**6**) [14] (7.03 g, 25.8 mmol) in MeOH (50 mL) was added $NaBH_4$ (3.88 g, 103 mmol) at 0 °C, and the resulting mixture was stirred at room temperature for 2 h. The reaction was quenched with H_2O (50 mL), and the aqueous mixture was extracted with CH_2Cl_2 (50 mL × 3). The organic extracts were combined, dried over $MgSO_4$. The solvent was removed under reduced pressure, and the residue was chromatographed on silica gel (40 g, hexane:acetone = 3:1) to give **7** (6.66 g, 95%) as a pale yellow oil: ^{1}H NMR (300 MHz, $CDCl_3$) δ: 1.26 (1H, br), 3.53 (3H, s), 5.01 (2H, s), 5.16 (2H, s), 5.24 (2H, s), 6.88–6.96 (2H, m), 7.16 (1H, d, J = 1.9 Hz), 7.30–7.45 (5H, m); ^{13}C NMR (75 MHz, $CDCl_3$) δ: 56.13, 64.64, 70.88, 95.40, 114.25, 116.22, 121.06, 126.98, 127.61, 128.27, 134.16, 136.82, 146.60, 148.19; IR (neat): 1511 (C=C), 3419 (OH) cm^{-1}; MS (EI) *m/z* 274 (M^+); HRMS (EI): calcd for $C_{16}H_{18}O_4$: 274.1205 (M^+), found: 274.1188.

*4.1.3.2. 2-(4-Benzyloxy-3-methoxymethoxybenzyl)malonic acid diethyl ester (**8**).* To a stirred solution of **7** (711 mg, 2.59 mmol) in CH_2Cl_2 (26 mL) were added NEt_3 (0.43 mL, 3.11 mmol) and MsCl (0.22 mL, 2.85 mmol) at 0 °C, and the reaction mixture was stirred at room temperature for 0.5 h. The reaction was quenched with sat. $NaHCO_3$ (aq) (20 mL), and the organic layer was separated. The aqueous layer was extracted with CH_2Cl_2 (30 mL × 3), and the organic layer and extracts were combined, dried over $MgSO_4$. The

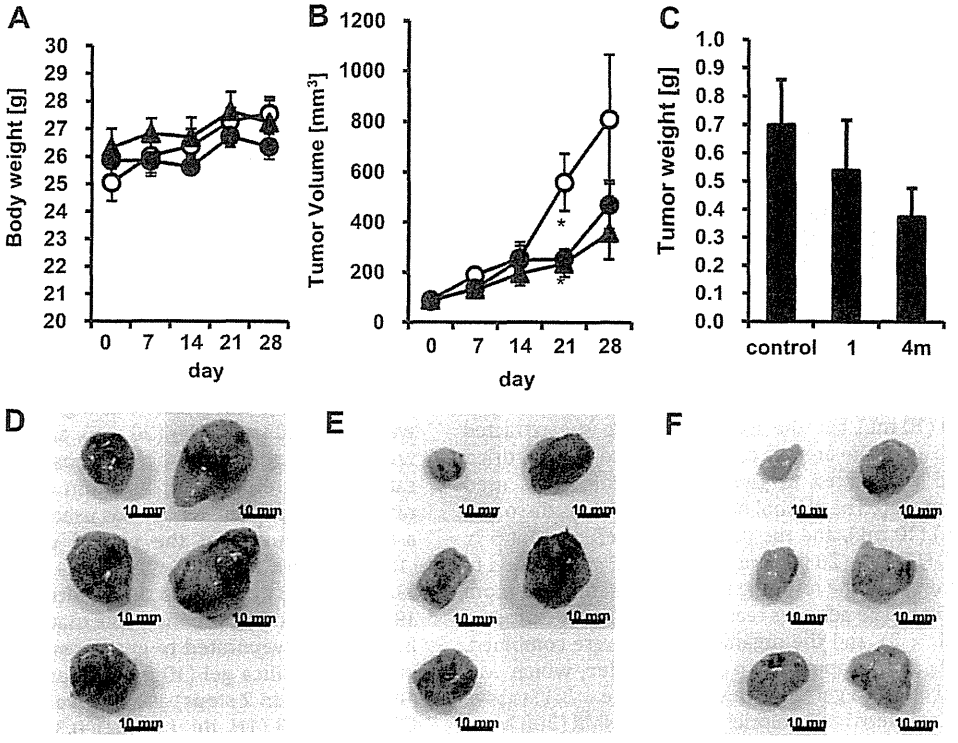

Fig. 4. Effect of triethoxy derivative **4m** and (−)-arctigenin (**1**) on the growth of CAPAN-1 cells in nude mice. A, body weight of mice. ○, control group (n = 5); ●, group treated with triethoxy derivative **4m** (n = 6); ▲, group treated with (−)-arctigenin (**1**) (n = 5). B, the tumor volume in the mice. ○, control group; ●, group treated with triethoxy derivative **4m**; ▲, group treated with (−)-arctigenin (**1**). C, wet weight of the tumor in the mice on the last day of the experiment. D–F, photographs of the tumor after sacrifice on the last day of control group, of group treated with (−)-arctigenin (**1**), and of group treated with triethoxy derivative **4m**, respectively.

solvent was removed under reduced pressure to give a pale yellow oil, which was used directly in the next step. To a stirred solution of diethyl malonate (0.79 mL, 5.18 mmol) in DMF (10 mL) was added NaH (60%, 207 mg, 5.18 mmol) at 0 °C, and the resulting mixture was stirred at room temperature for 1 h. To the solution was added a solution of the oil obtained above in DMF (2 mL) at 0 °C, and the reaction mixture was stirred at room temperature for 20 h. The reaction was quenched with sat. $NaHCO_3$ (aq) (10 mL), and the aqueous mixture was extracted with Et_2O (20 mL × 3). The organic extracts were combined, dried over $MgSO_4$, evaporated to give a pale yellow oil which was chromatographed on silica gel (20 g, hexane:acetone = 15:1) to give **8** (776 mg, 72% in 2 steps) as a pale yellow oil: ^{1}H NMR (300 MHz, $CDCl_3$) δ: 1.22 (6H, t, J = 7.1 Hz), 3.13 (2H, d, J = 7.6 Hz), 3.50 (3H, s), 3.60 (1H, t, J = 7.6 Hz), 4.16 (4H, q, J = 7.1 Hz), 5.11 (2H, s), 5.19 (2H, s), 6.74–6.83 (2H, m), 7.00 (1H, d, J = 1.7 Hz), 7.28–7.42 (5H, m); ^{13}C NMR (75 MHz, $CDCl_3$) δ: 14.05, 34.09, 53.93, 56.16, 61.35, 70.92, 95.64, 114.31, 117.98, 122.74, 127.01, 127.63, 128.31, 130.09, 136.95, 146.64, 147.71, 168.56; IR (neat): 1510 (C=C), 1732 (C=O) cm^{-1}; MS (EI) m/z 416 (M^+); HRMS (EI): calcd for $C_{23}H_{28}O_7$: 416.1835 (M^+), found: 416.1832.

*4.1.3.3. (R)-Acetic acid 3-(4-benzyloxy-3-methoxymethoxyphenyl)-2-hydroxymethylpropyl ester ((+)-**9**).* To a stirred solution of **8** (1.66 g, 3.98 mmol) in THF (40 mL) was added $LiAlH_4$ (378 mg, 9.96 mmol) at 0 °C, and the resulting suspension was refluxed for 12 h. The reaction was quenched with 10% NaOH (aq) (20 mL), and the mixture was extracted with AcOEt (20 mL × 5). The organic extracts were combined dried over $MgSO_4$, and the solvent was evaporated to give diol, which was used directly in the next step. To a stirred solution of the diol obtained above in i-Pr_2O–THF (20 mL, 4:1) were added lipase-PS (397 mg) and vinyl acetate (0.52 mL, 5.67 mmol), and the reaction mixture was stirred at room temperature for 2 h. The catalyst was filtered and the filtrate was evaporated to give residue, which was chromatographed on silica gel (30 g, hexane:acetone = 15:1) to give (+)-**9** (1.20 g, 80% in 2 steps) as a pale yellow oil. The enantiomeric excess of (+)-**9** was determined to be a 98% ee by the following HPLC analysis; chiralcel OJ (0.46 cm × 25 cm), hexane/2-propanol = 1/1, flow rate = 0.5 mL/min, λ = 254 nm, (+)-**9**; t_R = 29.7 min, (−)-**9**; 25.5 min ^{1}H NMR (300 MHz, $CDCl_3$) δ: 1.70 (1H, br), 2.09 (3H, s), 2.17 (1H, s), 2.55–2.62 (2H, m), 3.47–3.62 (2H, m), 3.52 (3H, s), 4.03–4.20 (2H, m), 5.13 (2H, s), 5.21 (2H, s), 6.72–6.98 (3H, m), 7.30–7.44 (5H, m); ^{13}C NMR (75 MHz, $CDCl_3$) δ: 20.99, 33.75, 42.47, 56.27, 62.08, 63.94, 71.14, 95.72, 114.534, 118.21, 122.92, 127.11, 127.71, 128.40, 132.46, 137.11, 146.82, 147.48, 171.47; IR (neat): 1739 (C=O), 3165 (OH) cm^{-1}; MS (EI) m/z 374 (M^+); HRMS (EI): calcd for $C_{21}H_{26}O_6$: 374.1729 (M^+), found: 374.1723; $[\alpha]_D^{26}$ +13.5 (c 1.14, $CHCl_3$).

*4.1.3.4. (R)-Acetic acid 3-(4-benzyloxy-3-methoxymethoxyphenyl)-2-methanesulfonyloxymethylpropyl ester (**10**).* To a stirred solution of (+)-**9** (666 mg, 1.78 mmol) in CH_2Cl_2 (8 mL) were added MsCl (0.15 mL, 1.95 mmol) and NEt_3 (0.32 mL, 2.31 mmol) at 0 °C, and the reaction mixture was stirred at room temperature for 0.5 h. The reaction was quenched with H_2O (8 mL), and the aqueous mixture was extracted with CH_2Cl_2 (10 mL × 3). The organic extracts were combined dried over $MgSO_4$, and evaporated. The residue was chromatographed on silica gel (30 g, hexane:acetone = 15:1) to give **10** (775 mg, 96%) as a pale yellow oil: ^{1}H NMR (300 MHz, $CDCl_3$) δ: 2.03 (3H, s), 2.27–2.34 (1H, m), 2.61 (2H, d, J = 7.42 Hz), 2.93 (3H, s), 3.47 (3H, s), 3.96–4.19 (4H, m), 5.08 (2H, s), 5.18 (2H, s), 6.69–6.95 (3H, m), 7.24–7.41 (5H, m); ^{13}C NMR (75 MHz, $CDCl_3$) δ: 20.91, 33.41, 37.26, 39.61, 56.29, 62.94, 68.34, 71.13, 95.67, 114.65, 118.05,

122.84, 127.12, 127.76, 128.42, 130.88, 136.98, 146.98, 147.72, 170.56; IR (KBr): 1242 (S=O), 1736 (C=O) cm^{-1}; MS (EI) *m/z* 452 (M^+); HRMS (EI): calcd for $C_{22}H_{28}O_8S$: 452.1505 (M^+), found: 452.1512; $[\alpha]_D^{25}$ +2.76 (*c* 1.40, $CHCl_3$).

*4.1.3.5. (R)-4-(4-Benzyloxy-3-hydeorxybenzyl)dihydrofuran-2-one (**11**).* To a stirred solution of **10** (993 mg, 2.19 mmol) in DMSO (20 mL) was added KCN (150 mg, 2.19 mmol), and the resulting mixture was heated at 90 °C for 3 h. After cooling, the reaction was quenched with H_2O (20 mL), and the aqueous mixture was extracted with Et_2O/AcOEt (1:1, 20 mL × 3). The organic extracts were combined, dried over $MgSO_4$, and evaporated to give cyanide, which was used directly in the next step. To a stirred solution of cyanide obtained above in THF–H_2O (3:1, 8 mL) was added LiOH·H_2O (91.9 mg, 2.19 mmol), and the reaction mixture was stirred at room temperature for 24 h. The reaction mixture was diluted with H_2O (10 mL), and the aqueous mixture was extracted with Et_2O (20 mL × 3). The organic extracts were combined, dried over $MgSO_4$, and evaporated to give alcohol, which was used directly in the next step. The alcohol obtained above was dissolved in 10% NaOH (aq) (10 mL), and the mixture was refluxed for 5 h. After cooling, 10% HCl (aq) (20 mL) and THF (20 mL) were added to the reaction mixture, and the resulting solution was stirred at room temperature for 50 h. The aqueous reaction mixture was extracted with Et_2O (30 mL × 3), and the organic extracts were combined, dried over $MgSO_4$, and evaporated to give a residue, which was chromatographed on silica gel (20 g, hexane:acetone = 3:1) to give **11** (479 mg, 73% in 4 steps) as a colorless solid: ^1H NMR (300 MHz, $CDCl_3$) δ: 2.17–2.32 (1H, m), 2.52–2.69 (3H, m), 2.74–2.86 (1H, m), 3.91–4.05 (1H, m), 4.30–4.36 (1H, m), 5.09 (2H, s), 5.67 (1H, br), 6.59–6.89 (3H, m), 7.36–7.85 (5H, m); ^{13}C NMR (75 MHz, $CDCl_3$) δ: 34.25, 37.22, 38.41, 71.22, 72.63, 112.26, 114.78, 120.04, 127.69, 128.32, 128.61, 131.72, 136.09, 144.50, 145.89, 176.68; IR (KBr): 1647 (C=O), 3445 (OH) cm^{-1}; MS (EI) *m/z* 298 (M^+); HRMS (EI): calcd for $C_{18}H_{18}O_4$: 298.1205 (M^+), found: 298.1204; $[\alpha]_D^{26}$ +5.6 (*c* 0.13, $CHCl_3$); mp: 137–139 °C.

*4.1.3.6. (R)-4-(4-Benzyloxy-3-methoxybenzyl)dihydrofuran-2-one (**12a**).* To a stirred solution of **11** (330 mg, 1.1 mmol) in acetone (15 mL) were added K_2CO_3 (168 mg, 1.2 mmol) and MeI (0.41 mL, 6.6 mmol), and the reaction mixture was refluxed for 24 h. After cooling, the insoluble materials were filtered, and the filtrate was evaporated to give a residue, which was chromatographed on silica gel (15 g, hexane:acetone = 4:1) to give **12a** (304 mg, 88%) as a colorless oil: ^1H NMR (300 MHz, $CDCl_3$) δ: 2.17 (2H, s), 2.24–2.30 (1H, m), 3.88 (3H, s), 4.03–4.05 (1H, m), 4.30–4.35 (1H, m), 5.13 (2H, s), 6.61–6.64 (2H, m), 6.81–6.83 (1H, m), 7.27–7.45 (5H, m); ^{13}C NMR (75 MHz, $CDCl_3$) δ: 34.29, 37.30, 38.64, 56.06, 71.11, 72.60, 112.32, 114.23, 120.52, 127.12, 127.72, 128.40, 131.25, 136.96, 146.91, 149.66, 176.65; IR (neat): 1654 (C=C), 1774 (C=O) cm^{-1}; MS (EI) *m/z* 312 (M^+); HRMS (EI): calcd for $C_{19}H_{20}O_4$: 312.1362 (M^+), found: 312.1380; $[\alpha]_D^{25}$ +4.9 (*c* 0.95, $CHCl_3$).

*4.1.3.7. (R)-4-(4-Benzyloxy-3-ethoxybenzyl)dihydrofuran-2-one (**12b**).* By the procedure similar to preparation of **12a**, **12b** was prepared from **11** and EtI (84%) as a pale yellow oil: ^1H NMR (300 MHz, $CDCl_3$) δ: 1.44 (3H, t, *J* = 4.4 Hz), 2.28 (1H, dd, *J* = 17.3, 6.9 Hz), 2.60 (1H, dd, *J* = 17.3, 8.0 Hz), 2.67–2.84 (3H, m), 4.02–4.13 (3H, m), 4.32 (1H, dd, *J* = 9.1, 6.9 Hz), 5.12 (2H, s), 6.60–6.69 (2H, m), 6.84 (1H, d, *J* = 8.2 Hz), 7.30–7.77 (5H, m); ^{13}C NMR (75 MHz, $CDCl_3$) δ: 15.03, 34.29, 37.31, 38.61, 64.74, 71.37, 72.62, 114.29, 115.22, 120.73, 127.08, 127.63, 128.34, 131.46, 137.20, 147.33, 149.18, 176.67; IR (neat): 1507 (C=C), 1772 cm^{-1} (C=O); MS (EI) *m/z* 326 (M^+); HRMS (EI): calcd for $C_{20}H_{22}O_4$: 326.1518 (M^+), found: 326.1523; $[\alpha]_D^{26}$ +3.4 (*c* 1.78, $CHCl_3$).

*4.1.3.8. (R)-4-(4-Benzyloxy-3-propoxybenzyl)dihydrofuran-2-one (**12c**).* By the procedure similar to preparation of **12a**, **12c** was prepared from **11** and *n*-PrBr (87%) as a colorless oil: ^1H NMR (600 MHz, $CDCl_3$) δ: 1.04 (3H, t, *J* = 7.0 Hz), 1.84 (2H, sextet, *J* = 7.0 Hz), 2.26 (1H, dd, *J* = 17.5, 7.0 Hz), 2.57 (1H, dd, *J* = 17.5, 8.1 Hz), 2.64–2.71 (2H, m), 2.74–2.83 (1H, m), 3.96 (2H, t, *J* = 7.0 Hz), 4.00 (1H, dd, *J* = 9.2, 5.9 Hz), 4.30 (1H, dd, *J* = 9.2, 7.0 Hz), 5.09 (2H, s), 6.60 (1H, d, *J* = 8.1 Hz), 6.67 (1H, s), 6.82 (1H, d, *J* = 8.1 Hz), 7.27–7.42 (5H, m); ^{13}C NMR (100 MHz, $CDCl_3$) δ: 10.46, 22.55, 34.07, 37.15, 38.43, 70.65, 71.32, 72.55, 114.28, 115.38, 120.69, 127.10, 127.63, 128.34, 131.61, 137.31, 147.37, 149.52, 176.84; IR (neat): 1508 (C=C), 1773 (C=O) cm^{-1}; MS (EI) *m/z* 340 (M^+); HRMS (EI): calcd for 340.1675 (M^+), found: 340.1667; $[\alpha]_D^{26}$ −1.0 (*c* 1.05, $CHCl_3$).

*4.1.3.9. (R)-4-(3,4-Dimethoxybenzyl)dihydrofuran-2-one (**13a**).* To a stirred solution of **12a** (302 mg, 0.97 mmol) in MeOH (5 mL) was added 20% $Pd(OH)_2$ (20 mg), and the resulting suspension was stirred under a hydrogen atmosphere at 1 atm for 15 h. The catalyst was removed by filtration and the filtrate was evaporated to give phenol, which was used directly in the next step. To a stirred solution of the phenol obtained above in acetone (10 mL) were added K_2CO_3 (201.1 mg, 1.46 mmol) and MeI (0.18 mL, 2.92 mmol), and the resulting mixture was refluxed for 19 h. After cooling, the insoluble materials were filtered, and the filtrate was evaporated to give a residue, which was chromatographed on silica gel (10 g, hexane:acetone = 4:1) to give **13a** (130 mg, 55% in 2 steps) as a pale yellow oil: ^1H NMR (300 MHz, $CDCl_3$) δ: 2.33 (1H, dd, *J* = 18.0, 9.3 Hz), 2.61 (1H, dd, *J* = 17.4, 8.1 Hz), 2.70–2.87 (3H, m), 3.87 (3H, s), 3.88 (3H, s), 4.05 (1H, dd, *J* = 9.3, 6.3 Hz), 4.33 (1H, dd, *J* = 9.3, 6.6 Hz), 6.66–6.72 (2H, m), 6.82 (1H, d, *J* = 8.1 Hz); $[\alpha]_D^{24}$ +22.2 (*c* 0.87, $CHCl_3$) (ref. [19], $[\alpha]_D^{25}$ +23.8).

*4.1.3.10. (R)-4-(4-Ethoxy-3-methoxybenzyl)dihydrofuran-2-one (**13b**).* By the procedure similar to preparation of **13a**, **13b** was prepared from **12a** and EtI (55% in 2 steps) as a pale yellow oil: ^1H NMR (300 MHz, $CDCl_3$) δ: 1.46 (3H, t, *J* = 7.1 Hz), 2.29 (1H, dd, *J* = 17.6, 6.9 Hz), 2.63 (1H, dd, *J* = 17.6, 8.0 Hz), 2.71–2.88 (3H, m), 3.86 (3H, s), 4.03 (1H, dd, *J* = 9.1, 6.9 Hz), 4.06 (2H, q, *J* = 7.1 Hz), 4.34 (1H, dd, *J* = 9.1, 6.9 Hz), 6.65–6.68 (2H, m), 6.81 (1H, d, *J* = 8.2 Hz); ^{13}C NMR (75 MHz, $CDCl_3$) δ: 14.92, 34.32, 37.36, 38.65, 55.98, 64.38, 72.63, 112.01, 112.84, 120.56, 130.59, 147.06, 149.26, 176.68; IR (neat): 1514 (C=C), 1778 (C=O) cm^{-1}; MS (EI) *m/z* 250 (M^+); HRMS (EI): calcd for $C_{14}H_{18}O_4$: 250.1205 (M^+), found: 250.1192; $[\alpha]_D^{24}$ +4.4 (*c* 1.66, $CHCl_3$).

*4.1.3.11. (R)-4-(3-Ethoxy-4-methoxybenzyl)dihydrofuran-2-one (**13c**).* By the procedure similar to preparation of **13a**, **13c** was prepared from **12b** and MeI (55% in 2 steps) as a pale yellow oil: ^1H NMR (300 MHz, $CDCl_3$) δ: 1.47 (3H, t, *J* = 6.9 Hz), 2.29 (1H, dd *J* = 17.3, 6.6 Hz), 2.61 (1H, dd, *J* = 17.3, 8.0 Hz), 2.67–2.87 (3H, m), 3.86(3H, s), 4.01–4.12 (3H, m), 4.34 (1H, dd, *J* = 9.1, 6.6 Hz), 6.62–6.69 (2H, m), 6.81 (1H, d, *J* = 8.0 Hz); ^{13}C NMR (75 MHz, $CDCl_3$) δ: 14.87, 34.24, 37.31, 38.54, 55.95, 64.35, 72.58, 111.61, 113.24, 120.54, 130.52, 148.01, 148.22, 176.63; IR (neat): 1541 (C=C), 1771 (C=O) cm^{-1}; MS (EI) *m/z* 250 (M^+); HRMS (EI): calcd for $C_{14}H_{18}O_4$: 250.1205 (M^+), found: 250.1207; $[\alpha]_D^{27}$ +4.4 (*c* 1.94, $CHCl_3$).

*4.1.3.12. (R)-4-(3,4-Diethoxybenzyl)dihydrofuran-2-one (**13d**).* By the procedure similar to preparation of **13a**, **13d** was prepared from **12b** and EtI (47% in 2 steps) as a pale yellow oil: ^1H NMR (300 MHz, $CDCl_3$) δ: 1.41–1.47 (6H, m), 2.28 (1H, dd, *J* = 17.3, 6.6 Hz), 2.59 (1H, dd, *J* = 17.3, 8.0 Hz), 2.67–2.86 (3H, m), 4.00–4.11 (5H, m), 4.32 (1H, dd, *J* = 9.3, 6.6 Hz), 6.64–6.67 (2H, m), 6.81 (1H, d, *J* = 8.5 Hz); ^{13}C NMR (75 MHz, $CDCl_3$) δ: 14.97, 34.30, 37.36, 38.61, 64.64, 64.69, 72.65,

113.70, 114.12, 120.78, 130.70, 147.53, 148.72, 176.68; IR (neat): 1507 (C=C), 1771 (C=O) cm^{-1}; MS (EI) *m/z* 264 (M^+); HRMS (EI): calcd for $C_{15}H_{20}O_4$: 264.1362 (M^+), found: 264.1369; $[\alpha]_D^{26}$ +5.4 (*c* 1.29, $CHCl_3$).

*4.1.3.13. (R)-4-(4-Methoxy-3-propoxybenzyl)dihydrofuran-2-one (**13e**).* By the procedure similar to preparation of **13a**, **13e** was prepared from **12c** and MeI (80% in 2 steps) as a pale yellow oil: ^1H NMR (400 MHz, $CDCl_3$) δ: 1.05 (3H, t, J = 7.1 Hz), 1.87 (2H, sextet, J = 7.1 Hz), 2.29 (1H, dd, J = 17.5, 6.8 Hz), 2.60 (1H, dd, J = 17.5, 8.1 Hz), 2.65–2.73 (2H, m), 2.77–2.84 (1H, m), 3.85 (1H, s), 3.96 (2H, t, J = 7.1 Hz), 4.03 (1H, dd, J = 9.3, 6.1 Hz), 4.33 (1H, dd, J = 9.3, 7.0 Hz), 6.67 (1H, s), 6.68 (1H, d, J = 7.8 Hz), 6.81 (1H, d, J = 7.8 Hz); ^{13}C NMR (100 MHz, $CDCl_3$) δ: 10.37, 22.44, 34.15, 37.23, 38.45, 56.00, 70.51, 72,57, 111.89, 113.52, 120.60, 130.67, 148.25, 148.62, 176.86; IR (neat): 1516 (C=C), 1778 (C=O) cm^{-1}; MS (EI) *m/z* 264 (M^+); HRMS(EI): calcd for $C_{15}H_{20}O_4$: 264.1362 (M^+), found: 264.1345; $[\alpha]_D^{26}$ +3.2 (*c* 1.05, $CHCl_3$).

*4.1.3.14. (R)-4-(4-Ethoxy-3-propoxybenzyl)dihydrofuran-2-one (**13f**).* By the procedure similar to preparation of **13a**, **13f** was prepared from **12c** and EtI (77% in 2 steps) as a pale yellow oil: ^1H NMR (400 MHz, $CDCl_3$) δ: 1.05 (3H, t, J = 7.0 Hz), 1,42 (3H, t, J = 6.8 Hz), 1.87 (2H, sextet, J = 7.0 Hz), 2.28 (1H, dd, J = 17.5, 7.0 Hz), 2.60 (1H, dd, J = 17.5, 8.0 Hz), 2.64–2.72 (2H, m), 2.74–2.85 (1H, m), 3.94 (2H, t, J = 7.0 Hz), 4.01–4.09 (3H, m), 4.32 (1H, dd, J = 9.1, 6.9 Hz), 6.64 (1H, s), 6.65 (1H, d, J = 8.0 Hz), 6.81 (1H, d, J = 8.0 Hz); ^{13}C NMR (100 MHz, $CDCl_3$) δ: 10.35, 14.79, 22.50, 34.10, 37.16, 38.38, 64.67, 70.72, 72.56, 114.05, 114.31, 120.78, 130.88, 147.64, 149.09, 176.85; IR (neat): 1510 (C=C), 1774 (C=O) cm^{-1}; MS (EI) *m/z* 278 (M^+); HRMS (EI): calcd for $C_{16}H_{22}O_4$: 278.1518 (M^+), found: 278.1512; $[\alpha]_D^{26}$ +1.2 (*c* 1.05, $CHCl_3$).

*4.1.3.15. (3R,4R)-3-(4-Benzyloxy-3-methoxybenzyl)-4-(3-ethoxy-4-methoxybenzyl)dihydrofuran-2-one (**14a**).* To a stirred solution of **13b** (29.6 mg, 0.12 mmol) in THF (2 mL) were added LiHMDS (1.6 M in THF, 0.12 mL, 0.18 mmol), HMPA (31 μL, 0.18 mmol) at −78 °C, and the resulting solution was stirred at the same temperature for 0.5 h. To the reaction mixture was added a solution of 4-benzyloxy-3-methoxybenzyl bromide [20] (52.3 mg, 0.19 mmol) in THF (2 mL), and allowed to warm to room temperature over 1 h, and then stirred at the same temperature for 20 h. The reaction was quenched with H_2O (4 mL), and the aqueous mixture was extracted with Et_2O (10 mL × 3). The organic extracts were combined, dried over $MgSO_4$, and evaporated to give residue, which was chromatographed on silica gel (10 g, hexane:acetone = 4:1) to give **14a** (25 mg, 44%) as a pale yellow oil: ^1H NMR (300 MHz, $CDCl_3$) δ: 1.44 (3H, t, J = 6.9 Hz), 2.46–2.65 (4H, m), 2.91–2.95 (2H, m), 3.79–3.90 (1H, m), 3.84 (6H, s), 4.01 (2H, q, J = 6.9 Hz), 4.08–4.20 (1H, m), 5.12 (2H, s), 6.50–6.80 (6H, m), 7.28–7.43 (5H, m); ^{13}C NMR (75 MHz, $CDCl_3$) δ: 14.77, 34.48, 38.02, 41.09, 46.42, 55.90, 64.28, 65.18, 71.03, 71.16, 111.57, 112.85, 113.35, 113.92, 114.02, 120.54, 121.28, 127.17, 127.20, 127.76, 128.46, 130.32, 130.82, 137.06, 147.01, 148.09, 148.26, 149.73, 178.65; IR (neat): 1515 (C=C), 1770 (C=O) cm^{-1}; MS (EI) *m/z* 476 (M^+); HRMS (EI): calcd for $C_{29}H_{32}O_6$: 476.2199 (M^+), found: 476.2197; $[\alpha]_D^{25}$ −16.4 (*c* 0.77, $CHCl_3$).

*4.1.3.16. (3R,4R)-3-(4-Benzyloxy-3-ethoxybenzyl)-4-(3-ethoxy-4-methoxybenzyl)dihydrofuran-2-one (**14b**).* By the procedure similar to preparation of **14a**, **14b** was prepared from **13b** and 4-benzyloxy-3-ethoxybenzyl bromide [21] (59%) as a pale yellow oil: ^1H NMR (300 MHz, $CDCl_3$) δ: 1.34–1.40 (6H, m), 2.36–2.51 (4H, m), 2.81–2.85 (2H, m), 3.71–3.78 (1H, m), 3.75 (3H, s), 3.90–4.05 (5H, m), 5.02 (2H, s), 6.40–6.80 (6H, m), 7.14–7.35 (5H, m); ^{13}C NMR (75 MHz, $CDCl_3$) δ: 14.75, 14.82, 34.43, 37.99, 41.05, 46.39, 55.86, 64.22, 64.47, 71.14, 71.26, 111.51, 113.24, 114.59, 114.97, 120.51, 121.39, 127.11, 127.64, 128.35, 130.31, 130.99, 137.27, 147.33, 148.03, 148.23, 149.24, 178.65; IR (neat): 1507 (C=C), 1771 (C=O) cm^{-1}; MS (EI) *m/z* 490 (M^+); HRMS (EI): calcd for $C_{30}H_{34}O_6$: 490.2355 (M^+), found: 490.2383; $[\alpha]_D^{26}$ −14.8 (*c* 1.46, $CHCl_3$).

*4.1.3.17. (3R,4R)-3-(4-Benzyloxy-3-methoxybenzyl)-4-(4-ethoxy-3-methoxybenzyl)dihydrofuran-2-one (**14c**).* By the procedure similar to preparation of **14a**, **14c** was prepared from **13c** and 4-benzyloxy-3-methoxybenzyl bromide [20] (43%) as a pale yellow oil: ^1H NMR (300 MHz, $CDCl_3$) δ: 1.45 (3H, t, J = 6.9 Hz), 2.47–2.63 (4H, m), 2.91–2.95 (2H, m), 3.84 (3H, s), 3.91 (3H, s), 3.91–3.95 (1H, m), 4.09 (2H, q, J = 6.9 Hz), 4.03–4.14 (1H, m), 5.16 (2H, s), 6.48–6.96 (6H, m), 7.28–7.45 (5H, m); ^{13}C NMR (75 MHz, $CDCl_3$) δ: 14.90, 34.58, 38.19, 41.13, 46.55, 55.98, 64.35, 65.29, 71.06, 110.88, 112.03, 112.82, 113.89, 113.97, 119.21, 120.44, 121.22, 127.69, 128.40, 130.26, 130.73, 134.03, 136.98, 146.91, 149.61, 178.49; IR (neat): 1261 (C=C), 1770 (C=O) cm^{-1}; MS (EI) *m/z* 476 (M^+); HRMS (EI): calcd for $C_{29}H_{32}O_6$: 476.2199 (M^+), found: 476.2209; $[\alpha]_D^{26}$ −9.0 (*c* 1.75, $CHCl_3$).

*4.1.3.18. (3R,4R)-3-(4-Benzyloxy-3-ethoxybenzyl)-4-(4-ethoxy-3-methoxybenzyl)dihydrofuran-2-one (**14d**).* By the procedure similar to preparation of **14a**, **14d** was prepared from **13c** and 4-benzyloxy-3-ethoxybenzyl bromide [21] (53%) as a pale yellow oil: ^1H NMR (300 MHz, $CDCl_3$) δ: 1.41–1.48 (6H, m), 2.44–2.67 (4H, m), 2.88–2.93 (2H, m), 3.79 (3H, s), 3.80–3.87 (1H, m), 4.02–4.14 (5H, m), 5.11 (2H, s), 6.45–6.96 (6H, m), 7.27–7.45 (5H, m); ^{13}C NMR (75 MHz, $CDCl_3$) δ: 14.62, 14.69, 30.69, 34.27 37.89, 40.87, 46.28, 55.66, 64.12, 64.35, 71.04, 71.12, 111.92, 112.61, 114.52, 114.84, 120.38, 121.31, 127.02, 127.52, 128.23, 130.29, 130.91, 137.17, 146.91, 147.20, 149.10, 178.55; IR (neat): 1515 (C=C), 1771 (C=O) cm^{-1}; MS (EI) *m/z* 490 (M^+); HRMS (EI): calcd for $C_{30}H_{34}O_6$: 490.2355 (M^+), found: 490.2383; $[\alpha]_D^{24}$ −17.9 (*c* 1.14, $CHCl_3$).

*4.1.3.19. (3R,4R)-3-(4-Benzyloxy-3-propoxybenzyl)-4-(3-ethoxy-4-methoxybenzyl)dihydrofuran-2-one (**14e**).* By the procedure similar to preparation of **14a**, **14e** was prepared from **13b** and 4-benzyloxy-3-propoxybenzyl bromide, prepared from 4-benzyl-3-propoxybenzaldehyde [22], (40%) as a pale yellow oil: ^1H NMR (400 MHz, $CDCl_3$) δ: 1.05 (3H, t, J = 7.1 Hz), 1.45 (3H, t, J = 7.8 Hz), 1.84 (2H, sextet, J = 7.1 Hz), 2.46–2.64 (4H, m), 2.86–2.99 (2H, m), 3.80–3.87 (4H, m), 3.94 (2H, t, J = 7.1 Hz), 4.00 (2H, q, J = 7.8 Hz), 4.06–4.11 (1H, m), 5.10 (2H, s), 6.48–6.82 (6H, m), 7.28–7.44 (5H, m); ^{13}C NMR (100 MHz, $CDCl_3$) δ: 10.47, 14.75, 22.56, 34.47, 38.00, 41.10, 46.40, 55.87, 64.25, 70.53, 71.35, 111.55, 113.29, 114.71, 115.25, 120.52, 121.37, 127.18, 127.57, 127.63, 128.33, 130.35, 131.126, 137.34, 147.40, 148.07, 148.26, 149.57, 178.64; IR (neat): 1514 (C=C), 1771 (C=O) cm^{-1}; MS (EI) *m/z* 504 (M^+); HRMS(EI): calcd for $C_{31}H_{36}O_6$: 504.2512 (M^+), found: 504.2538; $[\alpha]_D^{24}$ −10.7 (*c* 0.75, $CHCl_3$).

*4.1.3.20. (3R,4R)-3-(4-Benzyloxy-3-methoxybenzyl)-4-(3,4-diethoxybenzyl)dihydrofuran-2-one (**14f**).* By the procedure similar to preparation of **14a**, **14f** was prepared from **13d** and 4-benzyloxy-3-methoxybenzyl bromide [20] (48%) as a pale yellow oil: ^1H NMR (300 MHz, $CDCl_3$) δ: 1.41–1.59 (6H, m), 2.43–2.63 (4H, m), 2.91–2.95 (2H, m), 3.82–3.90 (1H, m), 3.85 (3H, s), 3.82–3.89 (1H, m), 3.97–4.12 (5H, m), 5.12 (2H, s), 6.49–6.80 (6H, m), 7.26–7.44 (5H, m); ^{13}C NMR (75 MHz, $CDCl_3$) δ: 14.85, 34.50, 38.07, 41.12, 46.50, 55.96, 64.59, 71.09, 71.21, 112.90, 113.63, 114.06, 114.20, 120.78, 121.33, 127.26, 127.81, 128.51, 130.50, 130.86, 137.12, 147.06, 147.60, 148.77, 149.76, 178.70; IR (neat): 1509 (C=C), 1772 (C=O) cm^{-1}; MS (EI) *m/z* 490 (M^+); HRMS (EI): calcd for $C_{30}H_{34}O_6$: 490.2355 (M^+), found: 490.2388; $[\alpha]_D^{25}$ −13.5 (*c* 0.98, $CHCl_3$).

*4.1.3.21. (3R,4R)-3-(4-Benzyloxy-3-ethoxybenzyl)-4-(3,4-diethoxybenzyl)dihydrofuran-2-one (**14g**).* By the procedure similar to preparation of **14a**, **14g** was prepared from **13d** and 4-benzyloxy-3-ethoxybenzyl bromide [21] (56%) as a pale yellow oil: ^1H NMR

(300 MHz, $CDCl_3$) δ: 1.41–1.44 (9H, m), 2.42–2.60 (4H, m), 3.82–3.86 (1H, m), 4.02–4.13 (7H, m), 5.11 (2H, s), 6.47–6.81 (6H, m), 7.27–7.44 (5H, m); ^{13}C NMR (75 MHz, $CDCl_3$) δ: 14.87, 34.50, 38.09, 41.11, 46.50, 64.60, 71.22, 71.37, 113.63, 114.17, 114.69, 115.08, 120.79, 121.48, 127.21, 127.71, 128.42, 130.53, 131.07, 137.35, 147.41, 147.95, 148.78, 149.32, 178.73; IR (neat): 1514 (C=C), 1770 (C=O) cm^{-1}; MS (EI) m/z 504 (M^+); HRMS (EI): calcd for $C_{31}H_{36}O_6$: 504.2512 (M^+), found: 504.6139; $[\alpha]_D^{25}$ −12.0 (c 0.58, $CHCl_3$).

*4.1.3.22. (3R,4R)-3-(4-Benzyloxy-3-propoxybenzyl)-4-(4-methoxy-3-propoxybenzyl)dihydrofuran-2-one (**14h**).* By the procedure similar to preparation of **14a**, **14h** was prepared from **13e** and 4-benzyloxy-3-propoxybenzyl bromide (49%) as a pale yellow oil: ^1H NMR (400 MHz, $CDCl_3$) δ: 1.02–1.08 (6H, m), 1.82–1.88 (4H, m), 2.45–2.63 (4H, m), 2.85–2.97 (2H, m), 3.83 (3H, s), 3.83–4.60 (6H, m), 5.10 (2H, s), 6.51–6.96 (6H, m), 7.28–7.45 (5H, m); ^{13}C NMR (100 MHz, $CDCl_3$) δ: 10.48, 14.84, 22.56, 34.46, 38.00, 41.07, 46.45, 64.71, 65.15, 70.55, 70.74, 71.18, 71.35, 71.37, 112.76, 114.42, 115.12, 119.34, 120.77, 121.40, 127.13, 127.15, 127.64, 128.34, 128.36, 130.63, 131.13, 137.36, 147.98, 149.58, 178.73; IR (neat): 1514 (C=C), 1771 (C=O) cm^{-1}; MS (EI) m/z 518 (M^+); HRMS(EI): calcd for $C_{32}H_{38}O_6$: 518.2668 (M^+), found: 518.2669; $[\alpha]_D^{25}$ −12.2 (c 0.75, $CHCl_3$).

*4.1.3.23. (3R,4R)-3-(4-Benzyloxy-3-propoxybenzyl)-4-(4-ethoxy-3-propoxybenzyl)dihydrofuran-2-one (**14i**).* By the procedure similar to preparation of **14a**, **14i** was prepared from **13f** and 4-benzyloxy-3-propoxybenzyl bromide (33%) as a pale yellow oil: ^1H NMR (400 MHz, $CDCl_3$) δ: 1.02–1.08 (6H, m), 1.41 (3H, t, J = 7.1 Hz), 1.80–1.91 (4H, m), 2.41–2.63 (4H, m), 2.87–2.94 (2H, m), 3.82–3.96 (5H, m), 4.01 (2H, q, J = 7.1 Hz), 4.05–4.10 (1H, m), 5.10 (2H, s), 6.49–6.96 (6H, m), 7.28–7.45 (5H, m); ^{13}C NMR (100 MHz, $CDCl_3$) δ: 10.50, 22.59, 34.51, 38.05, 41.12, 46.48, 56.00, 65.22, 70.57, 71.40, 111.86, 112.79, 113.63, 114.72, 115.30, 119.36, 120.55, 121.40, 127.16, 127.28, 127.65, 128.36, 130.41, 131.16, 137.37, 147.43, 148.25, 148.58, 149.62, 178.70; IR (neat): 1508 (C=C), 1767 (C=O) cm^{-1}; MS (EI) m/z 532 (M^+); HRMS (EI): calcd for $C_{33}H_{40}O_6$: 532.2825 (M^+), found: 518.2817; $[\alpha]_D^{25}$ −6.3 (c 0.80, $CHCl_3$).

*4.1.3.24. (3R,4R)-4-(3-Ethoxy-4-methoxybenzyl)-3-(4-hydroxy-3-methoxybenzyl)dihydrofuran-2-one (**4g**).* To a stirred solution of **14a** (47.5 mg, 0.10 mmol) in MeOH (5 mL) was added 20% $Pd(OH)_2$ (20 mg), and the resulting suspension was stirred under a hydrogen atmosphere at 1 atm for 20 h. The catalyst was removed by filtration and the filtrate was evaporated to give a residue, which was chromatographed on silica gel (10 g, hexane:acetone = 3:1) to give **4g** (34.1 mg, 89%) as a pale yellow oil: ^1H NMR (300 MHz, $CDCl_3$) δ: 1.45 (3H, t, J = 7.1 Hz), 2.43–2.65 (4H, m), 2.91–2.94 (2H, m), 3.81–3.89 (1H, m), 3.83 (3H, s), 3.84 (3H, s), 4.01 (2H, q, J = 7.1 Hz), 4.12 (1H, dd, J = 9.1, 6.9 Hz), 5.53 (1H, s), 6.47–6.65 (4H, m), 6.69 (1H, d, J = 8.0 Hz), 6.82 (1H, d, J = 8.0 Hz); ^{13}C NMR (75 MHz, $CDCl_3$) δ: 14.80, 30.91, 34.46, 38.09, 40.95, 46.55, 55.83, 55.94, 64.30, 71.27, 99.88, 111.54, 113.26, 114.10, 120.58, 122.08, 129.47, 130.35, 144.52, 146.67, 148.11, 148.33; IR (neat): 1513 (C=C), 1771 (C=O) cm^{-1}; MS (EI) m/z 386 (M^+); HRMS (EI): calcd for $C_{22}H_{26}O_6$: 386.1729 (M^+), found: 386.1693; $[\alpha]_D^{25}$ −17.2 (c 1.44, $CHCl_3$).

*4.1.3.25. (3R,4R)-4-(3-Ethoxy-4-hydroxybenzyl)-3-(3-ethoxy-4-methoxybenzyl)dihydrofuran-2-one (**4h**).* By the procedure similar to preparation of **4g**, **4h** was prepared from **14b** (63%) as a pale yellow oil: ^1H NMR (300 MHz, $CDCl_3$) δ: 1.42–1.47 (6H, m), 2.46–2.63 (4H, m), 2.92 (2H, d, J = 5.8 Hz), 3.81–3.89 (1H, m), 3.84 (3H, s), 3.97–4.12 (5H, m), 5.60 (1H, br), 6.48–6.84 (6H, m); ^{13}C NMR (75 MHz, $CDCl_3$) δ: 14.78, 30.88, 34.39, 38.04, 40.90, 46.53, 55.90, 64.26, 64.39, 71.24, 111.51, 112.37, 113.21, 114.01, 120.55, 121.95, 129.34, 130.35, 144.59, 145.93, 148.08, 148.03, 178.74; IR (neat): 1516 (C=C), 1768 (C=O) cm^{-1}; MS (EI) m/z 400 (M^+); HRMS (EI): calcd for $C_{23}H_{28}O_6$: 400.1886 (M^+), found: 400.1868; $[\alpha]_D^{27}$ −16.9 (c 1.13, $CHCl_3$).

*4.1.3.26. (3R,4R)-4-(4-Ethoxy-3-methoxybenzyl)-3-(4-hydroxy-3-methoxybenzyl)dihydrofuran-2-one (**4i**).* By the procedure similar to preparation of **4g**, **4i** was prepared from **14c** (57%) as a pale yellow oil: ^1H NMR (300 MHz, $CDCl_3$) δ: 1.45 (3H, t, J = 7.1 Hz), 2.44–2.67 (4H, m), 2.93 (2H, d, J = 5.8 Hz), 3.81 (3H, s), 3.82 (3H, s), 3.84–3.99 (1H, m), 4.03–4.15 (1H, m), 4.08 (2H, q, J = 7.1 Hz), 5.30 (1H, br), 6.47–6.66 (4H, m), 6.75 (1H, d, J = 8.0 Hz), 6.82 (1H, d, J = 8.0 Hz); ^{13}C NMR (75 MHz, $CDCl_3$) δ: 14.90, 30.99, 34.53, 38.22, 40.97, 46.63, 55.89, 64.35, 71.31, 111.48, 112.00, 112.71, 114.04, 120.47, 122.01, 129.37, 130.30, 144.39, 146.54, 146.99, 149.18, 178.56; IR (neat): 1749 (C=O), 3648 (OH) cm^{-1}; MS (EI) m/z 386 (M^+); HRMS (EI): calcd for $C_{22}H_{26}O_6$: 386.1729 (M^+), found: 386.1693; $[\alpha]_D^{26}$ −9.5 (c 0.71, $CHCl_3$).

*4.1.3.27. (3R,4R)-4-(3-Ethoxy-4-hydroxybenzyl)-3-(4-ethoxy-3-methoxybenzyl)dihydrofuran-2-one (**4j**).* By the procedure similar to preparation of **4g**, **4j** was prepared from **14d** (63%) as a pale yellow oil: ^1H NMR (300 MHz, $CDCl_3$) δ: 1.39–1.46 (6H, m), 2.41–2.66 (4H, m), 2.91 (2H, d, J = 6.0 Hz), 3.80 (3H, s), 3.81–3.87 (1H, m), 4.00–4.10 (5H, m), 5.64 (1H, br), 6.47–6.65 (4H, m), 6.74 (1H, d, J = 8.2 Hz), 6.82 (1H, d, J = 8.2 Hz); ^{13}C NMR (75 MHz, $CDCl_3$) δ: 14.75, 30.86, 34.35, 38.06, 40.84, 46.54, 55.78, 64.26, 64.37, 71.24, 111.98, 112.38, 112.69, 114.00, 120.52, 121.95, 129.32, 130.38, 144.58, 145.91, 147.07, 149.25; IR (neat): 1771 (C=O), 3548 (OH) cm^{-1}; MS (EI) m/z 400 (M^+); HRMS (EI): calcd for $C_{23}H_{28}O_6$: 400.1886 (M^+), found: 400.1897; $[\alpha]_D^{26}$ −12.4 (c 1.04, $CHCl_3$).

*4.1.3.28. (3R,4R)-4-(3-Ethoxy-4-methoxybenzyl)-3-(4-hydroxy-3-propoxybenzyl)dihydrofuran-2-one (**4k**).* By the procedure similar to preparation of **4g**, **4k** was prepared from **14e** (56%) as a pale yellow oil: ^1H NMR (400 MHz, $CDCl_3$) δ: 1.04 (3H, t, J = 7.4 Hz), 1.45 (3H, t, J = 7.1 Hz), 1.82 (2H, sextet, J = 7.4 Hz), 2.48–2.63 (4H, m), 2.91 (2H, d, J = 5.9 Hz), 3.81–3.88 (4H, m), 3.93 (2H, t, J = 7.4 Hz), 4.02 (2H, q, J = 7.1 Hz), 4.06–4.12 (1H, m), 5.57 (1H, s), 6.48 (1H, s), 6.54 (1H, d, J = 10.2 Hz), 6.60 (1H, d, J = 10.2 Hz), 6.66 (1H,s), 6.75 (1H, d, J = 8.2 Hz), 6.82 (1H, d, J = 8.2 Hz); ^{13}C NMR (100 MHz, $CDCl_3$) δ: 10.43, 14.79, 22.49, 34.41, 38.05, 40.95, 46.54, 55.92, 64.29, 70.32, 71.24, 111.55, 112.43, 113.26, 114.01, 120.57, 121.93, 129.37, 130.37, 144.64, 146.05, 148.12, 148.33, 178.75; IR (neat): 1516 (C=C), 1769 (C=O), 3589 (OH) cm^{-1}; MS (EI) m/z 414 (M^+); HRMS (EI): calcd for $C_{24}H_{30}O_6$: 414.2042 (M^+), found: 414.2046; $[\alpha]_D^{26}$ −10.6 (c 1.10, $CHCl_3$).

*4.1.3.29. (3R,4R)-4-(3,4-Diethoxybenzyl)-3-(4-hydroxy-3-methoxybenzyl)dihydrofuran-2-one (**4l**).* By the procedure similar to preparation of **4g**, **4l** was prepared from **14f** (81%) as a pale yellow oil: ^1H NMR (300 MHz, $CDCl_3$) δ: 1.25–1.45 (6H, m), 2.44–2.66 (4H, m), 2.92 (2H, d, J = 6.0 Hz), 3.83 (3H, s), 3.85–3.89 (1H, m), 3.98–4.13 (5H, m), 5.55 (1H, br), 6.49–6.67 (4H, m), 6.76 (1H, d, J = 7.8 Hz), 6.82 (1H, d, J = 7.8 Hz); ^{13}C NMR (75 MHz, $CDCl_3$) δ: 14.84, 30.91, 34.40, 38.04, 40.94, 46.56, 55.84, 64.58, 71.25, 111.56, 113.60, 114.11, 120.77, 122.10, 129.47, 130.51, 144.51, 146.65, 147.57, 148.78, 178.75; IR (neat): 1766 (C=O), 2978 (OH) cm^{-1}; MS (EI) m/z 400 (M^+); HRMS (EI): calcd for $C_{23}H_{28}O_6$: 400.1886 (M^+), found: 400.1858; $[\alpha]_D^{27}$ −16.0 (c 1.33, $CHCl_3$).

*4.1.3.30. (3R,4R)-4-(3,4-Diethoxybenzyl)-3-(4-hydroxy-3-ethoxybenzyl)dihydrofuran-2-one (**4m**).* By the procedure similar to preparation of **4g**, **4m** was prepared from **14g** (66%) as a pale yellow oil: ^1H NMR (300 MHz, $CDCl_3$) δ: 1.40–1.46 (9H, m), 2.42–2.67 (4H, m), 2.91 (2H, d, J = 5.7 Hz), 3.85 (1H, dd, J = 9.1, 7.4 Hz), 3.97–4.12

(7H, m), 5.59 (1H, br), 6.49–6.66 (4H, m), 6.75 (1H, d, J = 8.0 Hz), 6.82 (1H, d, J = 8.0 Hz); ^{13}C NMR (75 MHz, $CDCl_3$) δ: 14.81, 14.85, 34.39, 38.06, 40.92, 46.58, 64.42, 64.59, 71.27, 112.43, 113.62, 114.05, 114.10, 120.80, 122.00, 129.37, 130.53, 144.61, 145.94, 147.58, 148.80, 178.79; IR (neat): 1516 (C=C), 1761 (C=O) cm^{-1}; MS (EI) m/z 414 (M^+); HRMS (EI): calcd for $C_{24}H_{30}O_6$: 414.2042 (M^+), found: 414.2024; $[\alpha]_D^{25}$ −14.0 (c 0.70, $CHCl_3$).

*4.1.3.31. (3R,4R)-4-(4-Methoxy-3-propoxybenzyl)-3-(4-hydroxy-3-propoxybenzyl)dihydrofuran-2-one (**4n**).* By the procedure similar to preparation of **4g**, **4n** was prepared from **14h** (46%) as a pale yellow oil: ^{1}H NMR (400 MHz, $CDCl_3$) δ: 1.02–1.07 (6H, m), 1.78–1.90 (4H, m), 2.47–2.65 (4H, m), 2.92 (2H, d, J = 5.9 Hz), 3.81 (3H, s), 3.81–3.95 (5H, m), 4.08–4.12 (1H, m), 5.56 (1H, br), 6.50 (1H, s), 6.53 (1H, d, J = 7.9 Hz), 6.60 (1H, d, J = 7.9 Hz), 6.66 (1H, s), 6.75 (1H, d, J = 8.2 Hz), 6.82 (1H, d, J = 8.2 Hz); ^{13}C NMR (100 MHz, $CDCl_3$) δ:10.39, 22.45, 22.47, 34.37, 38.01, 40.91, 46.54, 56.00, 70.29, 70.48, 71.23, 77.21, 111.81, 112.43, 113.53, 114.00, 120.55, 121.90, 129.34, 130.41, 144.61, 146.03, 148.22, 148.58, 178.74; IR (neat): 1516 (C=C), 1767 (C=O), 3422 (OH) cm^{-1}; MS (EI) m/z 428 (M^+); HRMS (EI): calcd for $C_{25}H_{32}O_6$: 428.2199 (M^+), found: 428.2216; $[\alpha]_D^{25}$ −13.7 (c 0.70, $CHCl_3$).

*4.1.3.32. (3R,4R)-4-(4-Ethoxy-3-propoxybenzyl)-3-(4-hydroxy-3-propoxybenzyl)dihydrofuran-2-one (**4o**).* By the procedure similar to preparation of **4g**, **4o** was prepared from **14i** (63%) as a pale yellow oil: ^{1}H NMR (400 MHz, $CDCl_3$) δ: 1.02–1.07 (6H, m), 1.42 (3H, t, J = 7.1 Hz), 1.80–1.86 (4H, m), 2.41–2.63 (4H, m), 2.92 (2H, d, J = 5.9 Hz), 3.83–3.96 (5H, m), 4.01 (2H, q, J = 7.1 Hz), 4.07–4.11 (1H, m), 5.57 (1H, s), 6.51–6.84 (6H, m); ^{13}C NMR (100 MHz, $CDCl_3$) δ: 10.50, 22.59, 34.51, 38.05, 41.12, 46.48, 56.00, 65.22, 70.57, 71.40, 111.86, 112.79, 113.63, 114.72, 115.30, 119.36, 120.55, 121.40, 127.16, 127.28, 127.65, 128.36, 130.41, 131.16, 137.37, 147.43, 148.25, 148.58, 149.62, 178.7010.45, 14.87, 22.50, 22.60, 34.37, 38.04, 40.92, 46.58, 64,76, 70.33, 70.76, 71.26, 100.36, 112.48, 114.02, 114.06, 114.38, 129.37, 130.67, 144.63, 146.04, 147.70, 149.14; IR (neat): 1508 (C=C), 1770 (C=O) cm^{-1}; MS (EI) m/z 442 (M^+); HRMS (EI): calcd for $C_{26}H_{34}O_6$: 442.2355 (M^+), found: 442.2350; $[\alpha]_D^{25}$ −12.9 (c 0.50, $CHCl_3$).

*4.1.4. Effective synthesis of (3R,4R)-4-(3,4-diethoxybenzyl)-3-(4-hydroxy-3-ethoxybenzyl)dihydrofuran-2-one (**4m**)*

*4.1.4.1. 2-(3,4-Diehtoxybenzyl)malonic acid diethyl ester (**17**).* To a stirred solution of (3,4-diehtoxyphenyl)methanol (**16**) [16,23] (733 mg, 3.74 mmol) in CH_2Cl_2 (20 mL) were added NEt_3 (0.67 mL, 4.86 mmol) and MsCl (0.32 mL, 4.11 mmol) at 0 °C, and the reaction mixture was stirred at room temperature for 0.5 h. The reaction was quenched with sat. $NaHCO_3$ (aq) (10 mL), and the organic layer were separated. The aqueous layer was extracted with CH_2Cl_2 (20 mL × 3), and the organic layer and extracts were combined, dried over $MgSO_4$. The solvent was removed under reduced pressure to give a pale yellow oil, which was used directly in the next step. To a stirred solution of diethyl malonate (1.14 ml, 7.48 mmol) in DMF (20 mL) was added NaH (60%, 299 mg, 7.48 mmol) at 0 °C, and the resulting mixture was stirred at room temperature for 1 h. To the solution was added a solution of the oil obtained above in DMF (2 mL) at 0 °C, and the reaction mixture was stirred at room temperature for 25 h. The reaction was quenched with sat. $NaHCO_3$ (aq) (10 mL), and the aqueous mixture was extracted with Et_2O (20 mL × 3). The organic extracts were combined, dried over $MgSO_4$, evaporated to give a pale yellow oil which was chromatographed on silica gel (20 g, hexane:acetone = 15:1) to give **17** (1.10 g, 87% in 2 steps) as a pale yellow oil: ^{1}H NMR (300 MHz, $CDCl_3$) δ: 1.15–1.30 (6H, m), 1.39–1.46 (6H, m), 3.13 (2H, d, J = 8.0 Hz), 3.59 (1H, t, J = 8.0 Hz), 4.01–4.24 (8H, m), 6.68–6.78 (3H, m); ^{13}C NMR (75 MHz, $CDCl_3$) δ: 13.77, 13.83, 14.57, 14.60, 34.06, 41.37, 53.82, 61.11, 64.19, 113.33, 114.09, 120.83, 130.28, 147.28, 148.33, 166.34, 168.64; IR (neat): 1516 (C=C), 1731 (C=O) cm^{-1}; MS (EI) m/z 338 (M^+); HRMS (EI): calcd for $C_{23}H_{28}O_6$: 338.1729 (M^+), found: 338.1766.

*4.1.4.2. (R)-Acetic acid 3-(3,4-diethoxyphenyl-2-hydroxymethylpropyl ester (**18**).* To a stirred solution of **17** (1.43 g, 4.23 mmol) in THF (40 mL) was added $LiAlH_4$ (401 mg, 10.6 mmol) at 0 °C, and the resulting suspension was refluxed for 12 h. The reaction was quenched with 10% NaOH (aq) (20 mL), and the mixture was extracted with AcOEt (20 mL × 5). The organic extracts were combined dried over $MgSO_4$, and the solvent was evaporated to give diol, which was used directly in the next step. To a stirred solution of the diol obtained above in i-Pr_2O–THF (15 mL, 4:1) were added Lipase-PS (323 mg) and vinyl acetate (0.45 ml, 4.85 mmol), and the reaction mixture was stirred at room temperature for 2 h. The catalyst was filtered and the filtrate was evaporated to give residue, which was chromatographed on silica gel (30 g, hexane:acetone = 4:1) to give **18** (669 mg, 53% in 2 steps) as a pale yellow oil. The enantiomeric excess of **18** was determined to be a 98% ee by the Moscher's method [24]. ^{1}H NMR (300 MHz, $CDCl_3$) δ: 1.39–1.44 (6H, m), 2.06 (3H, s), 2.23 (1H, br), 2.49–2.64 (2H, m), 3.45–3.59 (2H, m), 4.01–4.08 (6H, m), 4.15 (1H, dd, J = 11.3, 4.7 Hz), 6.66–6.70 (2H, m), 6.78 (1H, d, J = 8.0 Hz); ^{13}C NMR (75 MHz, $CDCl_3$) δ: 14.88, 20.91, 33.86, 42.53, 62.07, 64.03, 64.55, 64.63, 113.69, 114.52, 121.22, 131.91, 147.23, 148.70, 171.68; IR (neat): 1513 (C=C), 1721 (C=O) cm^{-1}; MS (EI) m/z 296 (M^+); HRMS (EI): calcd for $C_{16}H_{24}O_5$: 296.1624 (M^+), found: 296.1594; $[\alpha]_D^{28}$ +18.8 (c 1.47, $CHCl_3$); 98% ee.

*4.1.4.3. (R)-Acetic acid 3-(3,4-Diethoxyphenyl-2-methanesulfonyloxymethylpropyl ester (**19**).* To a stirred solution of **18** (1.45 g, 4.96 mmol) in CH_2Cl_2 (25 mL) were added MsCl (0.42 ml, 5.45 mmol) and NEt_3 (0.89 ml, 6.45 mmol) at 0 °C, and the reaction mixture was stirred at room temperature for 0.5 h. The reaction was quenched with H_2O (20 mL), and the aqueous mixture was extracted with CH_2Cl_2 (20 mL × 3). The organic extracts were combined dried over $MgSO_4$, and evaporated. The residue was chromatographed on silica gel (40 g, hexane:acetone = 4:1) to give **19** (1.48 g, 79%) as a pale yellow oil: ^{1}H NMR (300 MHz, $CDCl_3$) δ: 1.41–1.46 (6H, m), 2.08 (3H, s), 2.32–2.36 (1H, m), 2.65 (2H, d, J = 7.4 Hz), 2.99 (3H, s), 4.00–4.23 (8H, m), 6.65–6.70 (2H, m), 6.80 (1H, d, J = 8.0 Hz); ^{13}C NMR (75 MHz, $CDCl_3$) δ: 14.85, 20.81, 30.90, 33.49, 37.21, 39.71, 63.02, 64.60, 68.48, 113.70, 114.40, 121.22, 130.36, 147.53, 148.82, 170.78; IR (neat): 1512 (C=C), 1735 (C=O) cm^{-1}; MS (EI) m/z 374 (M^+); HRMS (EI): calcd for $C_{17}H_{26}O_7S$: 374.1399 (M^+), found: 374.1362; $[\alpha]_D^{25}$ +2.1 (c 0.68, $CHCl_3$).

*4.1.4.4. (R)-4-(3,4-Diethoxybenzyl)dihydrofuran-2-one (**13d**) from **19**.* To a stirred solution of **19** (1.12 g, 3.00 mmol) in DMSO (25 mL) was added KCN (205 mg, 3.00 mmol), and the resulting mixture was heated at 90 °C for 3 h. After cooling, the reaction was quenched with H_2O (25 mL), and the aqueous mixture was extracted with Et_2O/AcOEt (1:1, 20 mL × 3). The organic extracts were combined, dried over $MgSO_4$, and evaporated to give cyanide, which was used directly in the next step. To a stirred solution of cyanide obtained above in THF–H_2O (3:1, 12 mL) was added $LiOH \cdot H_2O$ (126 mg, 3.00 mmol), and the reaction mixture was stirred at room temperature for 24 h. The reaction mixture was diluted with H_2O (10 mL), and the aqueous mixture was extracted with Et_2O (20 mL × 3). The organic extracts were combined, dried over $MgSO_4$, and evaporated to give alcohol, which was used directly in the next step. The alcohol obtained above was dissolved in 10% NaOH (aq) (15 mL), and the mixture was refluxed for 5 h. After cooling, 10% HCl (aq) (30 mL) and THF (30 mL) were added to

the reaction mixture, and the resulting solution was stirred at room temperature for 50 h. The aqueous reaction mixture was extracted with Et_2O (30 mL × 3), and the organic extracts were combined, dried over $MgSO_4$, and evaporated to give a residue, which was chromatographed on silica gel (30 g, hexane:acetone = 3:1) to give **13d** (475 mg, 60% in 3 steps) as a pale yellow oil.

4.2. In vitro preferential cytotoxicity

4.2.1. Cells and culture

Human pancreatic cancer cell lines, PANC-1 and CAPAN-1, were maintained in Dulbecco's modified Eagle's medium (DMEM, Nissui Pharmaceutical Co., Ltd., Tokyo, Japan) supplemented with 10% fetal bovine serum (FBS, Gibco BRL Products, Gaithersburg, MD, USA), 0.1% sodium bicarbonate (Nacalai Tesque Inc.), and 1% antibiotic-antimycotic solution (Sigma–Aldrich Inc., St. Louis, MO, USA). Nutrient deprived medium (NDM) contained 265 mg/L $CaCl_2 \cdot 2H_2O$, 0.1 mg/L $Fe(NO_3) \cdot 9H_2O$, 400 mg/L KCl, 200 mg/L $MgSO_4 \cdot 7H_2O$, 6400 mg/L NaCl, 700 mg/L $NaHCO_3$, 125 mg/L NaH_2PO_4, 15 mg/L phenol red, 1 M HEPES buffer (pH 7.4, Wako Pure Chemical Industries, Ltd., Osaka, Japan), and 10 mL MEM vitamin solution (Life Technologies, Inc., Rockville, MD, USA). The final pH was adjusted to 7.4 with 10% $NaHCO_3$. For amino acid supplementation, stock solutions (200 mmol/L L-glutamine solution, MEM amino acids solution, and MEM nonessential amino acids solution; Life Technologies) were added at a concentration of 1%.

4.2.2. Preferential cytotoxicity

Preferential cytotoxicity was determined as previously described [9]. In brief, PANC-1 or CAPAN-1 cells (2×10^4 cells/well) were seeded in 96-well plates (Corning Inc., Corning, NY, USA) and incubated in fresh DMEM at 37 °C under 5% CO_2 and 95% air for 24 h. The cells were washed with Dulbecco's phosphate-buffered saline (PBS, Nissui Pharmaceutical Co., Ltd., Tokyo, Japan) before the medium was replaced with either DMEM or NDM (for CAPAN-1, amino acids-supplimented NDM) containing serial dilutions of the test samples. After 24 h of incubation, the cells were washed with PBS, and 100 μL of DMEM containing 10% WST-8 cell counting kit solution (Dojindo, Kumamoto, Japan) was added to the wells. After 3 h of incubation, the absorbance was measured at 450 nm. Cell viability was calculated from the mean values for three wells using the following equation:

Cell viability (%) = [(Abs(test samples) − Abs(blank))/(Abs((control) − Abs(blank))] × 100

The preferential cytotoxicity was expressed as the concentration at which 50% of cells died preferentially in NDM (PC_{50}).

4.3. In vivo antitumor activity of triethoxy derivative **4m** in nude mice

Five-week-old female BALB/cAJcl-*nu/nu* mice were obtained from CLEA Japan, Inc. (Tokyo, Japan), and 5×10^6 CAPAN-1 cells in 0.3 mL DMEM were s.c. injected into the right side of the back of the animals. Two weeks later, 12 mice bearing tumors around 5 mm in diameter were randomly divided into treatment groups and a vehicle control group. Because (−)-arctigenin (**1**) and triethoxy derivative **4m** are poorly soluble in water, they were first dissolved in DMSO at 10 mg/mL and kept frozen until use. Just before administration, the stock solution was diluted in saline to a final concentration of 250 μg/mL (the final concentration of DMSO in saline is 2.5%). The mice were administered by *i.p.*-injections of 0.2 mL of solution of arctigenin, triethoxy derivative **4m**, or vehicle on 6 days of the week for 4 weeks. The tumor size and body weight were measured weekly and the tumor volume was calculated using the following formula: Tumor volume = $4/3 \times 3.14 \times (L/2 \times W/2 \times W/2)$ where L is the length of the tumor and W is its width. Results are expressed as means ±SD. Statistical comparisons were conducted using Student's t test after ANOVA. The results were considered to be significant when $P < 0.05$.

Acknowledgments

This work was supported in part by grants from the Ministry of Health and Welfare for the Third-Term Comprehensive 10-Year Strategy for Cancer Control and by Grant-in-Aid for Scientific Research (C) (No. 22590098) from Japan Society for the Promotion of Science (JSPS).

Appendix A. Supplementary data

Supplementary data related to this article can be found at http://dx.doi:10.1016/j.ejmech.2012.11.031H.

References

[1] J. Ferlay, H.R. Shin, F. Bray, D. Forman, C. Mathers, D.M. Parkin, GLOBOCAN 2008 v1.2, Cancer Incidence and Mortality Worldwide: IARC CancerBase No. 10 (Internet), International Agency for Research on Cancer, Lyon, France, 2010, Available from:, http://globocan.iarc.fr (accessed 08.05.12).
[2] D. Li, K. Xie, R. Wolff, J.L. Abbruzzese, Pancreatic cancer, Lancet 363 (2004) 1049–1057.
[3] S. Shore, D. Vimalachandran, M.G.T. Raraty, P. Ghaneh, Cancer in the elderly: pancreatic cancer, Surg. Oncol. 13 (2004) 201–210.
[4] H.W. Chung, S.M. Bang, S.W. Park, J.B. Chung, J.K. Kang, J.W. Kim, J.S. Seong, W.J. Lee, S.Y. Song, A prospective randomized study of gemcitabine with doxifluridine versus pacritaxel with doxifluridine in concurrent chemo-radiotherapy for locally advanced pancreatic cancer, Int. J. Radiat. Oncol. 60 (2004) 1494–1501.
[5] C.V. Dang, G.L. Semenza, Oncogenic alteration of metabolism, Trends Biochem. Sci. 24 (1999) 68–72.
[6] M. Kitano, M. Kudo, K. Maekawa, Y. Suetomi, H. Sakamoto, N. Fukuta, R. Nakaoka, T. Kawasaki, Dynamic imaging of pancreatic diseases by contrast enhanced coded phase inversion harmonic ultrasonography, Gut 53 (2004) 854–859.
[7] K. Izuishi, K. Kato, T. Ogura, T. Kinoshita, H. Esumi, Remarkable tolerance of tumor cells to nutrient deprivation: possible new biochemical target for cancer therapy, Cancer Res. 60 (2000) 6201–6207.
[8] (a) H. Esumi, J. Lu, Y. Kurashima, T. Hanaoka, Antitumor activity of pyrvinium pamoate, 6-(dimethylamino)-2-[2-(2,5-dimethyl-1-phenyl-1*H*-pyrrol-3-yl) ethenyl]-1-methyl-quinolinium pamoate salt, showing preferential cytotoxicity during glucose starvation, Cancer Sci. 95 (2004) 685–690;
(b) J. Lu, S. Kunimoto, Y. Yamazaki, M. Kaminishi, H. Esumi, D. Kigamicin, A novel anticancer agent based on a new anti-austerity strategy targeting cancer cells' tolerance to nutrient starvation, Cancer Sci. 95 (2004) 547–552.
[9] S. Awale, J. Lu, S.K. Kalauni, Y. Kurashima, Y. Tezuka, S. Kadota, H. Esumi, Identification of arctigenin as an antitumor agent having the ability to eliminate the tolerance of cancer cells to nutrient starvation, Cancer Res. 66 (2006) 1751–1757.
[10] (a) B. Hausott, H. Greger, B. Marian, Naturally occurring lignans efficiently induce apoptosis in colorectal tumor cells, J. Cancer Res. Clin. Oncol. 129 (2003) 569–576;
(b) T. Matsumoto, K. Hosono-Nishiyama, H. Yamada, Antiproliferative and apoptotic effects of butyrolactone lignans from *Arctium lappa* on leukemic cells, Planta Med. 72 (2006) 276–278;
(c) T. Toyoda, T. Tsukamoto, T. Mizoshita, S. Nishibe, T. Deyama, Y. Takenaka, N. Hirano, H. Tanaka, S. Takasu, H. Ban, T. Kumagai, K. Inada, H. Utsunomiya, M. Tatematsu, Inhibitory effect of nordihydroguaiaretic acid, a plant lignan, on *Helicobacter pylori*-associated gastric carcinogenesis in Mongolian gerbils, Cancer Sci. 98 (2007) 1689–1695.
[11] (a) M. Nose, T. Fujimoto, T. Takeda, S. Nishibe, Y. Ogihara, Structural transformation of lignan compounds in rat gastrointestinal tract, Planta Med. 58 (1992) 520–523;
(b) S. Heinonen, T. Nurmi, K. Liukkonen, K. Poutanen, K. Wähälä, T. Deyama, S. Nishibe, H. Adlercreuta, In vitro metabolism of plant lignans: new precursors of mammalian lignans enterolactone and enterodiol, J. Agr. Food Chem. 49 (2001) 3178–3186;
(c) L.-H. Xie, E.-M. Ahn, T. Akao, A.A. Abdel-Hafez, N. Nakamura, M. Hattori, Transformation of arctiin to estrogenic and antiestrogenic substances by human intestinal bacteria, Chem. Pharm. Bull. 51 (2003) 378–384.
[12] E. Eich, H. Pertz, M. Kaloga, J. Schulz, M.R. Fesen, A. Mazumder, Y. Pommier, (−)-Arctigenin as a lead structure for inhibitors of human immunodeficiency virus type-1 integrase, J. Med. Chem. 39 (1996) 86–95.
[13] M.G. Banwell, S. Chand, G.P. Savage, An enantioselective total synthesis of the stilbenolignan (−)-aiphanol and the determination of its absolute stereochemistry, Tetrahedron: Asymmetry 16 (2005) 1645–1654.

[14] R. Fumeaux, C. Menozzi-Smarrito, A. Stalmach, C. Munari, K. Kraehenbuehl, H. Steiling, A. Crozier, G. Williamson, D. Barron, First synthesis, characterization, and evidence for the presence of hydroxycinnamic acid sulfate and glucuronide conjugates in human biological fluids as a result of coffee consumption, Org. Biomol. Chem. 8 (2010) 5199–5211.
[15] T. Cardinaels, J. Ramaekers, P. Nockemann, K. Driesen, K. Van Hecke, L. Van Meervelt, S. Lei, S. De Feyter, D. Guillon, B. Donnio, K. Binnemans, Imidazo[4,5-f]-1,10-phenanthrolines: versatile ligands for the design of metallomesogens, Chem. Mater. 20 (2008) 1278–1291.
[16] T.C. Daniels, R.E. Lyons, Ethyl esters of triiodophenoxyacetic acids and potassium triiodophenoxyacetate, J. Am. Chem. Soc. 58 (1936) 2646.
[17] M. Lieber, J. Mazzetta, W. Nelson-Rees, M. Kaplan, G. Todaro, Establishment of a continuous tumor-cell line (PANC-1) from a human carcinoma of the exocrine pancreas, Int. J. Cancer 15 (1975) 741–747.
[18] (a) H. Suemizu, M. Monnai, Y. Ohnishi, M. Ito, N. Tamaoki, M. Nakamura, Identification of a key molecular regulator of liver metastasis in human pancreatic carcinoma using a novel quantitative model of metastasis in NOD/SCID/γ_c^{null} (NOG) mice, Int. J. Oncol. 31 (2007) 741–751;
(b) A.P. Kyriazis, A.A. Kyriazis, D.G. Scarpelli, J. Fogh, M.S. Rao, R. Lepera, Human pancreatic adenocarcinoma line Capan-1 in tissue culture and the nude mouse. Morphologic, biologic, and biochemical characteristics, Am. J. Pathol. 106 (1982) 250–260.
[19] S. Koul, B. Singh, S.C. Taneja, G.N. Qazi, New chemo and chemo-enzymatic synthesis of β-benzyl-γ-butyrolactones, Tetrahedron 59 (2003) 3487–3491.
[20] A. Van Oeveren, J.F.G.A. Jansen, B.L. Feringa, Enantioselective synthesis of natural dibenzylbutyrolactone lignans (−)-enterolactone, (−)-hinokinin, (−)-pluviatolide, (−)-enterodiol, and furofuran lignan (−)-eudesmin via tandem conjugate addition tp g-alkoxybutenolides, J. Org. Chem. 59 (1994) 5999–6007.
[21] Aurora Building Blocks, Order Number: A00. 384. 218.
[22] B. Pelcman, J.G.K. Yee, L.F. Macenzie, Y. Zhou, K. Han, Isochromenones as PDE4 and PDE7 inhibitors and their preparation and use in the treatment of inflammation, PCT Int. Appl., 2010076564, 2010.
[23] (a) A. Enoki, M.H. Gold, Degradation of the diarylpropane lignin model compound 1-(3′,4′-diethoxyphenyl)-l,3-dihydroxy-2-(4′″-methoxyphenyl)-propane and derivatives by the basidiomycete *Phanerochaete chrysosporium*, Arch. Microbiol. 132 (1982) 123–130;
(b) V.C. Farmer, M.E.K. Henderson, J.D. Russel, Reduction of certain aromatic acids to aldehydes and alcohols by *Polystictus versicolor*, Biochim. Biophys. Acta 35 (1959) 202–211.
[24] J.A. Dale, S.H. Mosher, Nuclear magnetic resonance enantiomer regents. Configurational correlations via nuclear magnetic resonance chemical shifts of diastereomeric mandelate, O-methylmandelate, and α-methoxy-α-trifluoromethylphenylacetate (MTPA) esters, J. Am. Chem. Soc. 95 (1973) 512–519.

Drug Design, Development and Therapy

Dovepress

ORIGINAL RESEARCH

(+)-Grandifloracin, an antiausterity agent, induces autophagic PANC-1 pancreatic cancer cell death

Jun-ya Ueda[1,2]
Sirivan Athikomkulchai[3]
Ryuta Miyatake[4]
Ikuo Saiki[2]
Hiroyasu Esumi[5,6]
Suresh Awale[1,2]

[1]Frontier Research Core for Life Sciences, [2]Institute of Natural Medicine, University of Toyama, Toyama, Japan; [3]Faculty of Pharmacy, Srinakharinwirot University, Nakhon Nayok, Thailand; [4]Graduate School of Science and Engineering, University of Toyama, Toyama, Japan; [5]Research Institute for Biomedical Sciences, Tokyo University of Science, [6]National Cancer Center Hospital East, Chiba, Japan

Abstract: Human pancreatic tumors are known to be highly resistant to nutrient starvation, and this prolongs their survival in the hypovascular (austere) tumor microenvironment. Agents that retard this tolerance to nutrient starvation represent a novel antiausterity strategy in anticancer drug discovery. (+)-Grandifloracin (GF), isolated from *Uvaria dac*, has shown preferential toxicity to PANC-1 human pancreatic cancer cells under nutrient starvation, with a PC_{50} value of 14.5 μM. However, the underlying mechanism is not clear. In this study, GF was found to preferentially induce PANC-1 cell death in a nutrient-deprived medium via hyperactivation of autophagy, as evidenced by a dramatic upregulation of microtubule-associated protein 1 light chain 3. No change was observed in expression of the caspase-3 and Bcl-2 apoptosis marker proteins. GF was also found to strongly inhibit the activation of Akt, a key regulator of cancer cell survival and proliferation. Because pancreatic tumors are highly resistant to current therapies that induce apoptosis, the alternative cell death mechanism exhibited by GF provides a novel therapeutic insight into antiausterity drug candidates.

Keywords: (+)-grandifloracin, antiausterity strategy, PANC-1, nutrient starvation

Introduction

Human pancreatic cancer is the most fatal form of cancer worldwide, with a 5-year survival rate of less than 5%.[1] Each year, approximately 29,000 people are diagnosed with pancreatic cancer in Japan.[2] The annual mortality rate from this malignancy closely approximates the annual incidence rate.[3,4] Once diagnosed, the average life expectancy is 6 months. It is the fifth leading cause of cancer-related mortality in Japan and other industrialized countries.[4] Until now, no effective treatment has been available.[5,6] Human pancreatic cancer shows resistance to most conventional chemotherapeutic drugs in clinical use, such as paclitaxel, doxorubicin, and cisplatin.[7] At present, gemcitabine and S-1 (tegafur + gimeracil + oteracil potassium) are the only standard regimens for advanced pancreatic cancer.[8–11] Therefore, effective chemotherapeutic agents against this disease are urgently needed. Human pancreatic tumors are hypovascular in nature,[12] causing a limited supply of nutrients and oxygen to reach the aggressively proliferating tumor cells.[13] As tumor cells proliferate, the demand for essential nutrients and oxygen exceeds the supply. Consequently, large areas of tumor survive under the hostile environment characterized by nutrient and oxygen starvation. Yet, human pancreatic tumor cells show the extraordinary ability to tolerate such extreme states through the modulation of energy metabolism.[14] While normal human cells die within 24 hours under nutrient starvation, some human pancreatic cancer cell lines can survive up to 72 hours in the complete absence of nutrients such as glucose, amino acids, and serum.[14]

Correspondence: Suresh Awale
Frontier Research Core for Life Sciences, University of Toyama, 2630 Sugitani, Toyama 930-0194, Japan
Tel +81 76 434 7640
Fax +81 76 434 7640
Email suresh@inm.u-toyama.ac.jp

This remarkable tolerance to nutrient starvation is one of the key factors for survival and progression of pancreatic tumors. Therefore, agents that retard the tolerance of cancer cells to nutrient starvation represent a novel approach in anticancer drug discovery.[15] Using this hypothesis, we established a novel antiausterity strategy for the discovery of anticancer agents that preferentially target tolerance to nutrient starvation by cancer cells. Previous work on this strategy has led to the discovery of a number of potent anticancer agents, such as arctigenin,[15] angelmarin,[16] kayeassamins A–I,[17,18] and panduratins,[19,20] from the medicinal plants used in Japanese Kampo medicine and Southeast Asian countries.[21] Interestingly, these compounds also strongly suppressed tumor growth in a xenograft model using pancreatic cancer cells.[15] In our continued work, we recently found that a dichloromethane extract of the stem of *Uvaria dac* preferentially inhibited PANC-1 human pancreatic cancer cell survival under nutrient deprivation.[22] Work-up of this bioactive extract led to the discovery of (+)-grandifloracin (GF) as a potent antiausterity agent that showed preferential toxicity to PANC-1 cells with a PC_{50} value of 14.5 μM. In this study, we explored the underlying mechanism of GF-induced modulation of key regulatory proteins involved in tolerance to nutrient starvation in PANC-1 cells.

Materials and methods

Reagents

GF (Figure 1) was isolated from the stems of *U. dac* as described previously.[22] GF purity was determined to be 95% by high-performance liquid chromatography. Conventional anticancer agents, ie, gemcitabine, 5-fluorouracil, 2-deoxyglucose, paclitaxel, podophyllotoxin, and camptothecin, were purchased from Sigma-Aldrich (St Louis, MO, USA). Each reagent was dissolved in dimethyl sulfoxide as a 10 mM stock solution and stored at −30°C until use. Dilution to give the desired concentration was performed prior to treatment. Dulbecco's phosphate-buffered saline was purchased from Nissui Pharmaceutical (Tokyo, Japan). Dulbecco's Modified Eagle's Medium. (DMEM) was purchased from Wako Pure Chemical (Osaka, Japan). Sodium bicarbonate, potassium chloride, magnesium sulfate, sodium dihydrogen phosphate, potassium dihydrogen phosphate, sodium chloride, and phenol red were purchased from Wako Pure Chemical. HEPES was purchased from Dojindo Laboratories (Kumamoto, Japan). Fetal bovine serum was purchased from Nichirei Biosciences Inc. (Tokyo, Japan). Antibiotic/antimycotic solution was purchased from Sigma-Aldrich. The WST-8 cell counting kit was purchased from Dojindo Laboratories. Cell culture flasks and 96-well plates were obtained from Falcon Becton Dickinson Labware (BD Biosciences, San Jose, CA, USA). Nutrient-deprived medium was prepared according to a previously described protocol.[14] Rabbit polyclonal antibodies to Akt, phosphoryl Akt (Ser473), mammalian target of rapamycin (mTOR), phosphoryl mTOR (Ser2448), Bcl-2, caspase 3, and LC3A/B were purchased from Cell Signaling Technology (Danvers, MA, USA). A goat polyclonal antibody to actin was purchased from Santa Cruz Biotechnologies (Dallas, TX, USA). Horseradish peroxidase-conjugated goat polyclonal anti-rabbit and rabbit polyclonal anti-goat immunoglobulins were purchased from DakoCytomation (Glostrup, Denmark).

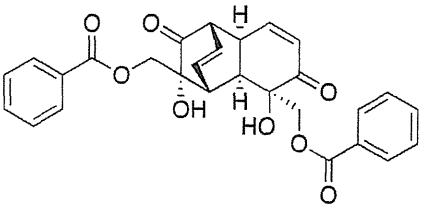

Figure 1 Chemical structure of (+)-grandifloracin.

Cell line

The PANC-1 (RBRC-RCB2095) cell line was purchased from the Riken BRC Cell Bank (Ibaraki, Japan) and maintained in standard DMEM with 10% fetal bovine serum supplement, 100 U/mL of penicillin G, 0.1 mg/mL of streptomycin, and 0.25 μg/mL of amphotericin B.

Preferential cytotoxic activity

The in vitro preferential cytotoxicity of GF was determined using a previously described procedure with a slight modification.[22] In brief, human pancreatic cancer cells were seeded in 96-well plates (1.5×10^4/well) and incubated in fresh DMEM at 37°C under humidified 5% CO_2 and 95% air for 24 hours. After the cells were washed with Dulbecco's phosphate-buffered saline, the medium was changed to serially diluted test samples in DMEM or nutrient-deprived medium, with the control and blank in each plate. After 24 hours of incubation, 100 μL of DMEM containing 10% WST-8 cell counting kit solution was directly added to each well. After 3 hours of incubation, absorbance at 450 nm was measured (EnSpire® Multilabel Reader, PerkinElmer, Waltham, MA, USA). Cell viability was calculated from the mean values for three wells using the following equation:

$$\text{Cell viability (\%)} = [(\text{Abs}_{(\text{test sample})} - \text{Abs}_{(\text{blank})})/(\text{Abs}_{(\text{control})} - \text{Abs}_{(\text{blank})})] \times 100$$

Morphologic assessment

Cells were seeded in 60 mm dishes (1×10^6 cells) and incubated in a humidified CO_2 incubator for 24 hours to allow cell attachment. The cells were then washed twice with Dulbecco's phosphate-buffered saline and treated with 25 μM GF in DMEM, nutrient-deprived medium, and the control. After 12 and 24 hours of incubation, the cells were treated with fluorescein-labeled annexin V and propidium iodide, and cell morphology was observed using an inverted Nikon Eclipse TS 100 microscope (40× objective) with phase-contrast and fluorescence modes. Microscopic images were taken using a Nikon DS-L-2 camera directly attached to the microscope.

Annexin V/dead cell assay

The annexin V/dead cell assay was performed in a Muse™ cell analyzer (Merck Millipore, Billerica, MA, USA) utilizing a Muse annexin V and dead cell kit. The assay utilizes phycoerythrin-labeled annexin V to detect phosphatidylserine on the external membrane of apoptotic cells. The kit contains the DNA dye, 7-aminoactinomycin D (7-AAD) for the exclusion of nonviable cells. Four populations of cells can be distinguished in this assay: nonapoptotic cells, annexin V (–) and 7-AAD (–); early apoptotic cells, annexin V (+) and 7-AAD (–); late-stage apoptotic and dead cells, annexin V (+) and 7-AAD (+); and necrotic nuclear debris, annexin V (–) and 7-AAD (+). The assay was performed according to the manufacturer's protocol. In brief, the cells were seeded in 60 mm dishes (1×10^6 cells) and incubated in a humidified CO_2 incubator for 24 hours to allow cell attachment. The cells were then washed twice with Dulbecco's phosphate-buffered saline and treated with 12.5 μM GF, 25 μM GF, or the control of nutrient-deprived medium for the indicated time periods. The cells were then harvested from the dish with trypsin to give single cell suspensions. Finally, 100 μL of annexin V/dead reagent and 100 μL of a single cell suspension were mixed in a microtube and incubated for 20 minutes at room temperature in the dark. The cells were then analyzed using the Muse cell analyzer, and 5,000 cell events were collected for each sample. The images were acquired as the screenshots of the processed data and the text size was edited for clarity.

Western blot analysis

Proteins were separated by gel electrophoresis on a polyacrylamide gel containing 0.1% sodium dodecyl sulfate and transferred to polyvinylidene fluoride membranes. The membranes were blocked with Block Ace® (DS Pharma Medical, Suita, Japan), washed with Dulbecco's phosphate-buffered saline containing 0.1% polyoxyethylene (20) sorbitan monolaurate (Wako Pure Chemical), and incubated overnight with primary antibodies diluted in Can Get Signal® (Toyobo, Osaka, Japan). After washing, the membranes were incubated for 45 minutes at room temperature with horseradish peroxidase-conjugated anti-rabbit or anti-goat immunoglobulins as the secondary antibody. The bands were detected with an enhanced chemiluminescence solution (PerkinElmer). The images were analyzed using Image Studio software version 3.1.4.

Statistical analysis

Statistical analysis was performed using the unpaired Student's *t*-test. A P-value<0.05 was considered to be statistically significant.

Results

GF showed preferential cytotoxicity in a concentration-dependent manner

The PANC-1 cell line is highly resistant to nutrient deprivation and shows an extraordinary ability to survive for >48 hours even under complete nutrient starvation. GF remarkably diminished tolerance to nutrient starvation in a concentration-dependent manner (Figure 2A). Cells exposed to GF at 25 μM showed 100% cell death within 24 hours in nutrient-deprived medium, with a PC_{50} value of 14.5 μM; however, no toxicity was observed in nutrient-rich DMEM.

GF sensitized PANC-1 cell death under glucose/serum-deprived conditions

To determine the conditions under which GF induces sensitivity to nutrient starvation resulting in cell death, the PANC-1 cells were treated with 25 μM GF under various nutrient conditions of glucose, amino acids, and serum. Cell viability was measured 24 hours after treatment. As shown in Figure 2B, GF was found to be toxic during glucose or serum deprivation, irrespective of the presence or absence of amino acids. In the presence of glucose and serum, cell viability was 100%. However, removal of serum led to a decrease in cell viability to 73% and 69% in the presence or absence of amino acids, respectively. Similarly, removal of glucose also led to a significant decrease in cell viability to 66%. Removal of both glucose and serum decreased cell viability to 2%.

Conventional anticancer agents are ineffective against PANC-1 cells in nutrient-deprived medium

The preferential cytotoxicity of GF was compared with that of several conventional anticancer agents, including

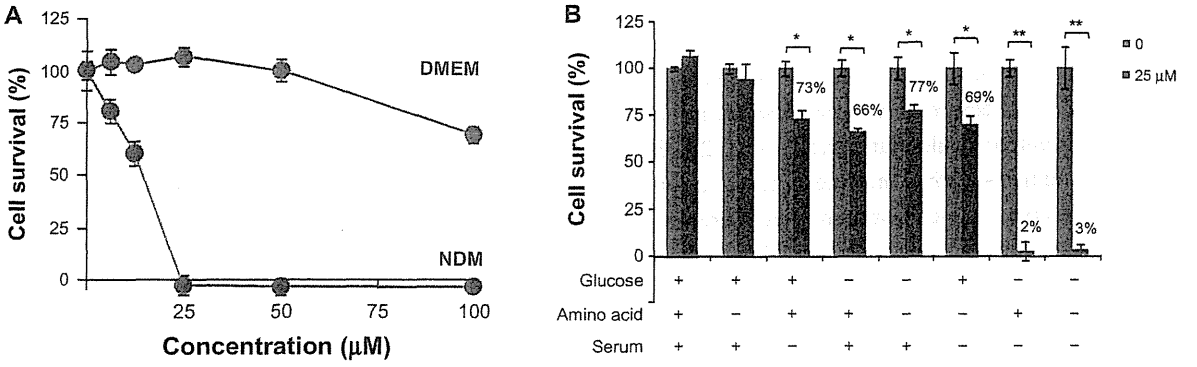

Figure 2 Effect of (+)-grandifloracin on PANC-1 cell survival after 24 hours in NDM and normal medium (DMEM). (**A**) Effect of (+)-grandifloracin concentration on cell survival in NDM and DMEM. (**B**) Effects of medium components, ie, glucose, amino acids, and serum. Data are expressed as the mean ± standard deviation, n=3. *$P<0.05$; **$P<0.01$ indicate significant difference from the control.
Abbreviations: NDM, nutrient-deprived medium; DMEM, Dulbecco's Modified Eagle's Medium.

gemcitabine, 5-fluorouracil, 2-deoxyglucose, paclitaxel, camptothecin, and podophyllotoxin, using PANC-1 cells grown in nutrient-deprived medium versus DMEM (Figure 3). All tested agents were virtually inactive in nutrient-deprived medium; however, paclitaxel and camptothecin showed weak activity in nutrient-rich DMEM at the maximum tested dose of 100 μM after 24 hours. Because some of the conventional anticancer agents showed weak activity in DMEM, their effects during prolonged treatment were also evaluated by monitoring their cytotoxicity after 24, 48, and 72 hours. As shown in Figure 4, gemcitabine and 5-fluorouracil weakly decreased cell viability 72 hours after treatment. However, these compounds did not show a clear concentration-dependent effect. 2-Deoxyglucose was completely inactive. Paclitaxel and podophyllotoxin were found to reduce cell viability after 72 hours, but the effect was not concentration-dependent. On the other hand, camptothecin exhibited strong activity with cell viability of <25% at 10 μM 48 hours after treatment.

Assessment of GF-induced apoptosis

To investigate whether GF-induced cell death in nutrient-deprived medium involves apoptosis, the cell morphology was examined. As shown in Figure 5, at 25 μM, GF induced a marked change in PANC-1 cell morphology within 8 hours. However, the cells lacked the classical signs of apoptosis, such as shrinkage or fragmentation into membrane-bound apoptotic bodies. Instead, swelling and rupture of cell membranes and disruption of cellular organelles appeared to be closer to a necrotic-type cell death. Staining with annexin V/propidium iodide reagent showed an increased population of cells containing Annexin V (green fluorescence) and propidium iodide (red fluorescence). Annexin V is a Ca^{2+}-dependent phospholipid-binding protein with

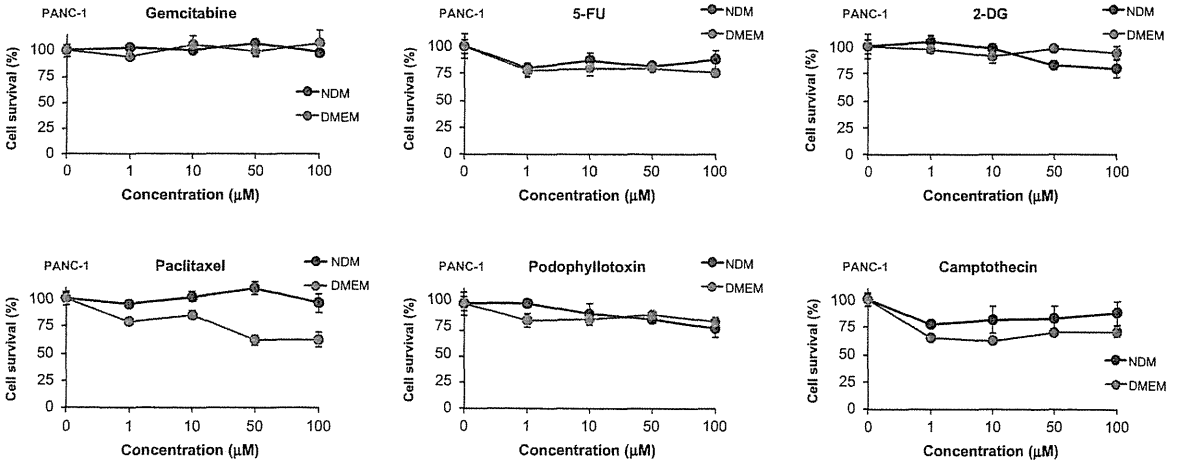

Figure 3 Effect of conventional anticancer agents against PANC-1 cells after 24 hours in NDM and DMEM. Data are expressed as the mean ± standard deviation, n=3.
Abbreviations: NDM, nutrient-deprived medium; DMEM, Dulbecco's Modified Eagle's Medium; 5-FU, 5-fluorouracil; 2-DG, 2-deoxyglucose.

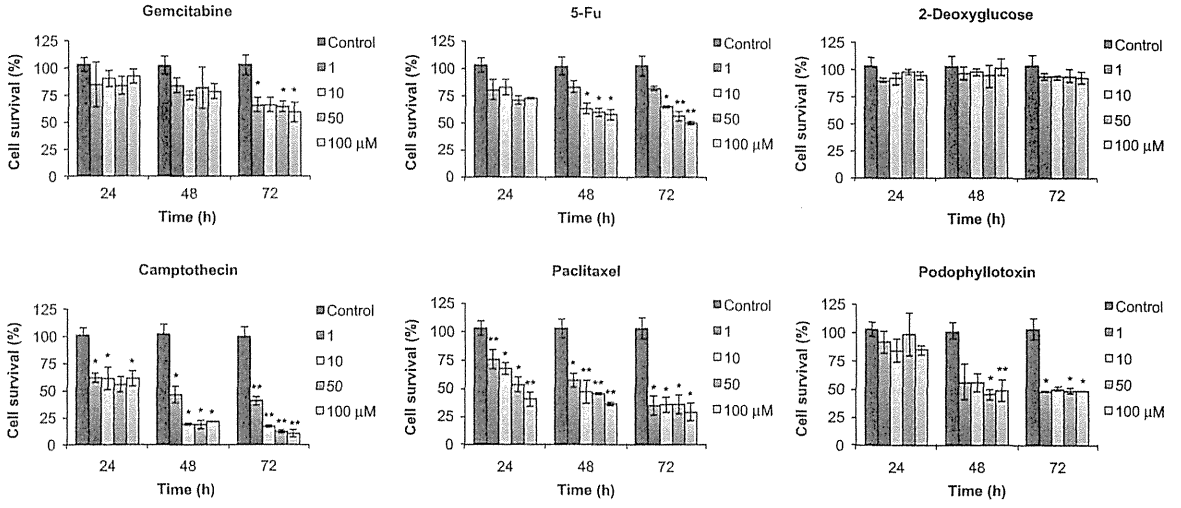

Figure 4 Assessment of cytotoxicity of conventional anticancer agents against PANC-1 cells in Dulbecco's Modified Eagle's Medium. Data are expressed as the mean ± standard deviation, n=3. *$P<0.05$; **$P<0.01$ indicates a significant difference from the control.
Abbreviation: 5-FU, 5-fluorouracil.

high affinity for phosphatidylserine. Translocation of phosphatidylserine to the external cell surface occurs both in apoptosis and necrosis. We further performed flow cytometric analysis of cells treated with GF utilizing the Muse Annexin V and dead cell kit, which contains 7-AAD as a dye for exclusion of nonviable cells. 7-AAD is impermeable to viable cells and does not stain viable or early apoptotic cells. In late apoptotic and necrotic cells, the integrity of the cell membrane decreases, which allows 7-AAD to pass through the membranes, intercalate into nucleic acids and DNA, and display red fluorescence. As shown in Figure 6, the cells are predominantly stained with both Annexin V and 7-AAD within 12 hours in a concentration-dependent manner. In the control of nutrient-deprived medium, more than 90% of the cells survived. After treatment with GF, this cell population decreased markedly to 72% (12.5 μM) and 29% (25 μM), with an increase in the late apoptotic/necrotic cell population from 1% (control) to 15% (12.5 μM) and 61% (25 μM), respectively (Figure 6). We further performed Western blot analysis to examine GF-induced apoptosis. Treatment with GF neither led to cleavage of caspase-3 nor showed Bcl-2 inhibition (data not shown).

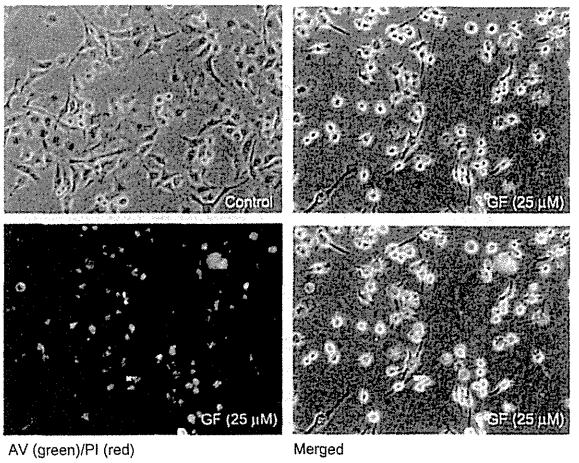

Figure 5 Effect of GF (25 μM) on PANC-1 cell morphology after 8 hours in NDM. Phase-contrast (upper left), fluorescent (lower left), and merged (lower right) images of PANC-1 cells.
Abbreviations: AV, Annexin V; PI, propidium iodide; NDM, nutrient-deprived medium; GF, (+)-grandifloracin.

GF inhibits Akt/mTOR activation

Akt is a prosurvival factor that is activated in a majority of tumors and regulates cellular functions such as cell cycle progression, cell migration, invasion, and angiogenesis. High Akt activation has been associated with tolerance to nutrient starvation and survival in an austerity environment.[14] Therefore, the effect of GF on Akt activation was investigated by Western blot analysis. As shown in Figure 6, Akt phosphorylation at Ser473 was completely inhibited by GF in a concentration-dependent as well as time-dependent manner in nutrient-deprived medium. GF also strongly suppressed total Akt. mTOR is a downstream effector of Akt and is frequently activated in various cancer types, where it is involved in tumor progression and metastasis.[23] Therefore, we tested whether GF has any modulatory activity against mTOR activation. As shown in Figure 7, addition of 25 μM GF completely inhibited mTOR phosphorylation at Ser2448 6 hours after treatment.

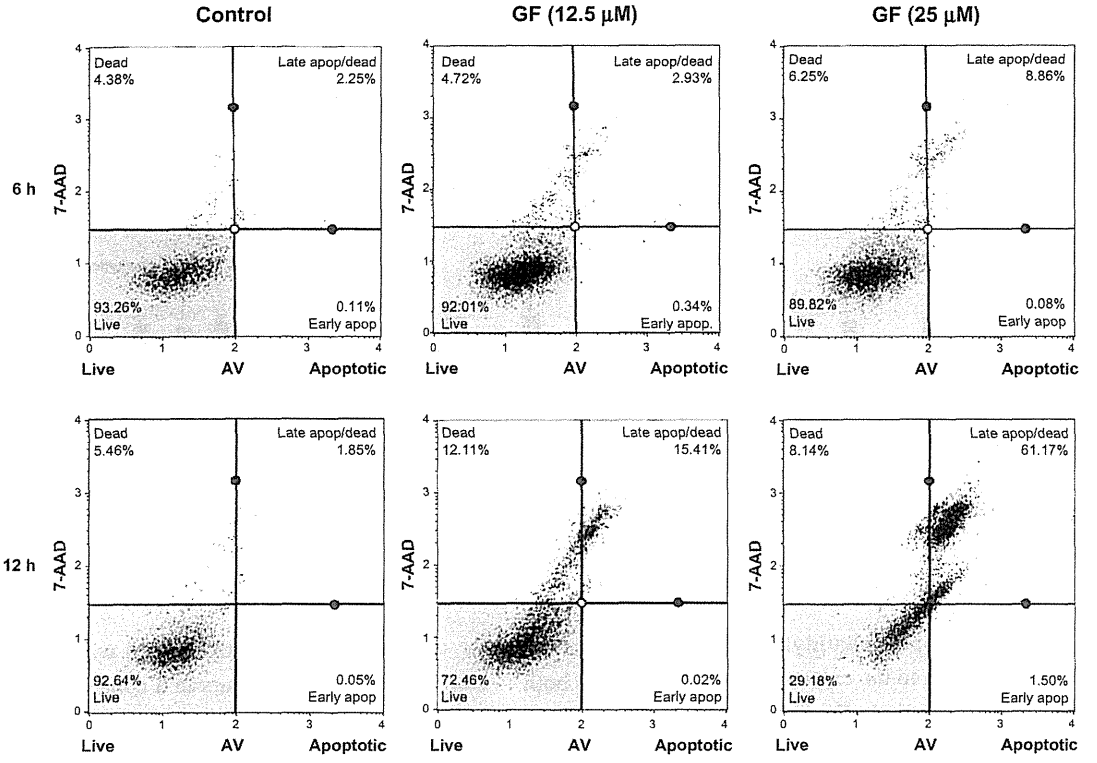

Figure 6 Assessment of apoptosis by GF. PANC-1 cells were treated with vehicle or GF (12.5 μM and 25 μM) in nutrient-deprived medium. After treatment (6 hours and 12 hours), the cells were treated with Annexin V/7-AAD reagent and cytometric analysis was performed.
Abbreviations: Apop, apoptotic; AV, Annexin V; GF, (+)-grandifloracin; 7-AAD; 7-aminoactinomycin D.

GF-induced autophagy in PANC-1 cells

Because no apoptotic cell death was observed in cells treated with GF, we speculated that GF might have induced autophagy. Therefore, expression of the autophagic marker microtubule-associated protein-light chain 3 (LC3), the cytoplasmic form of LC3-I (16 kDa), and the preautophagosomal and autophagosomal membrane-bound form of LC3-II (14 kDa) was examined by Western blot. The PANC-1 cells were cultured for varying time periods at different GF concentrations. As shown in Figure 7, no apparent differences were observed in LC3-I

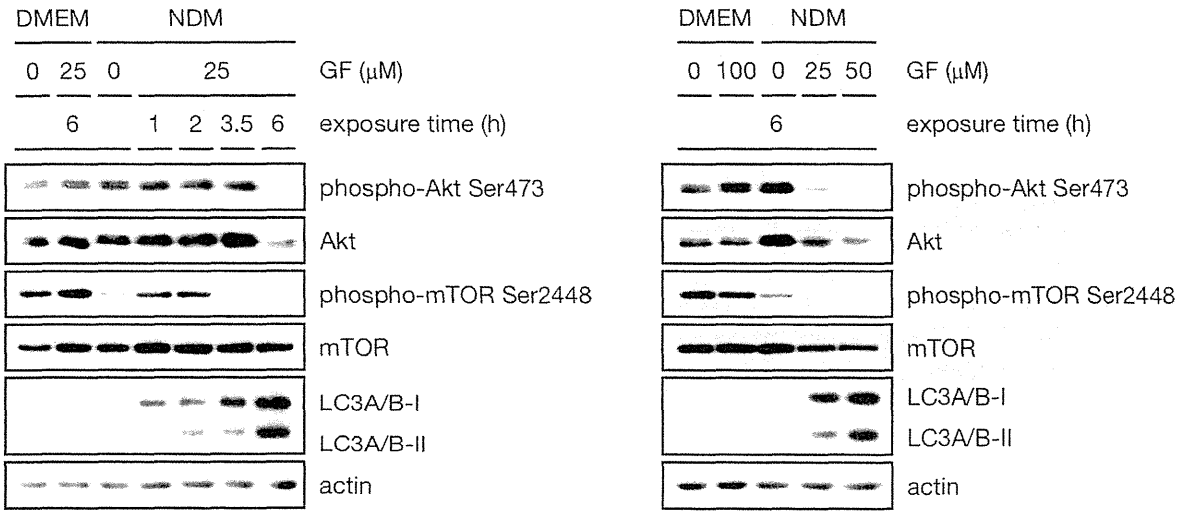

Figure 7 Effect of GF against Akt, mTOR, LC3A/B I, and LC3A/B II.
Abbreviations: GF, (+)-grandifloracin; NDM, nutrient-deprived medium; DMEM, Dulbecco's Modified Eagle's Medium.

and LC3-II expression in the controls of both DMEM and nutrient-deprived medium. However, treatment with GF led to an enhancement in the expression of both LC3-I and LC3-II in a concentration-dependent as well as time-dependent manner. In nutrient-deprived medium, treatment with 25 μM GF led to incremental increases of eight-fold, 13-fold, and 22-fold in LC3-I expression with respect to the control after 2, 3.5, and 6 hours, respectively. Similarly, increases of 141-fold, 146-fold, and 659-fold in LC3-II expression were observed with respect to the control after 2, 3.5, and 6 hours, respectively.

Discussion

Pancreatic cancer is associated with the lowest 5-year survival rate of any known cancer and is largely resistant to conventional chemotherapeutic agents. Although the median survival rate of the disease is only 6 months, some recent progress has been reported with FOLFIRINOX (folinic acid + 5-fluorouracil + irinotecan + oxaliplatin) and erlotinib.[24,25] However, new alternatives are urgently needed to improve the clinical outcome for patients diagnosed with pancreatic cancer. Pancreatic tumors are hypovascular and supply only a limited amount of essential nutrients and oxygen to aggressively proliferating cells. Consequently, these cells live in a hostile microenvironment under chronic metabolic stress conditions. For survival, these cells activate adaptive mechanisms such as autophagy.[26,27]

Autophagy is a homeostatic and evolutionarily conserved cellular pathway whereby cellular proteins and organelles are engulfed by autophagosomes, digested in lysosomes, and recycled in order to sustain cellular metabolism.[28] The process is activated in response to nutrient and energy starvation and acts as a survival mechanism to cope with diverse stresses in the tumor microenvironment.[28] Autophagy has been reported to be activated in colorectal cancer cells and to contribute to the tolerance to nutrient deprivation.[29] However, in the clinical setting, autophagy has been reported to serve as an alternative mechanism of programmed cell death that leads to tumor suppression.[30] One of the notable examples of a proautophagic cytotoxic drug that has demonstrated therapeutic benefits in several apoptosis-resistant cancer types in a clinical trial is temozolomide.[30] Several mechanisms have been suggested to explain the role of autophagy in suppression of tumorigenesis. Maintenance of genomic stability by clearance of damaged mitochondria and protein aggregates is considered one of the major mechanisms of tumor suppression by autophagy.[31] Further, excessive metabolic stresses in the tumor microenvironment often lead to necrotic cell death. Activation of autophagy under such circumstances prevents necrotic cell death and suppresses inflammation, which is known to increase tumor growth. Because the therapeutic goal of cancer treatment has been to trigger tumor-selective cell death, accelerating autophagy in apoptosis-resistant cancer cells would be an attractive alternative strategy in cancer therapy.

In the present study, GF does not appear to induce apoptosis but rather to operate by an alternative mechanism of programmed cell death, ie, autophagy. A marked activation of the autophagy marker LC3-II was observed after treatment with GF in a concentration-dependent and time-dependent manner. This was observed not only under nutrient-deprived conditions but also under nutrient-rich conditions, suggesting that GF is indeed an activator of autophagy. However, the effect of GF in nutrient-deprived medium was found to be highly significant compared with that in the control of nutrient-deprived medium at concentrations of 25 μM and 50 μM within 6 hours. Although a basal level of LC3-II protein is observed in the control of nutrient-deprived medium, it is activated within one hour after treatment with GF, which was found to be hyperactivated with respect to time as shown in Figure 5. This suggests that GF-induced autophagy mediates the death of PANC-1 cells preferentially during nutrient starvation.

The serine/threonine kinase Akt/mTOR pathway is constitutively activated in a majority of human pancreatic cancer cell lines. Activation of this pathway has been attributed to the survival of cancer cells in the heterogeneous tumor microenvironment, which confers resistance to chemotherapy and radiotherapy.[14] Akt has been found to be overexpressed in pancreatic cancer cells during extreme nutrient deprivation. Increased Akt expression is one of the austerity markers that enables tumor cells to survive and proliferate in the hostile hypovascular tumor microenvironment.[14] Therefore, inhibition of the Akt pathway might have therapeutic value in cancer patients. A number of antiausterity agents such as arctigenin, kigamicin D, and pyrvinium pamoate have been found to strongly suppress Akt activation, which suggests that inhibition of Akt phosphorylation by these compounds is partially responsible for the preferential cytotoxicity observed under nutrient deprivation.[15,32,33] However, the manner in which Akt inhibition affects downstream signaling under austerity conditions remains largely unknown. In the present study, GF suppressed both total Akt and phospho(Ser473) Akt in a time-dependent as well as concentration-dependent manner. It has been reported that mTOR is frequently inappropriately activated in many cancer types, and development of drugs that inhibit mTOR is an alluring therapeutic target in cancer therapy. mTOR is a downstream effector of the PI3K/AKT pathway and is composed of two distinct complexes,

ie, mTORC1 and mTORC2. In the present study, although the effects of GF on each multiprotein complex were not elucidated, complete inhibition of mTOR phosphorylation at Ser2448 was observed. mTOR inhibitors, such as temsirolimus and everolimus, have been approved by the US Food and Drug Administration for the treatment of renal cell carcinoma, primitive neuroectodermal tumor, and giant cell astrocytoma.[34] In this regard, GF is a dual inhibitor of the principal survival factors, Akt and mTOR, in tumors. Because pancreatic tumors are highly resistant to current chemotherapeutic agents that induce apoptosis, induction of an alternative cell death mechanism exhibited by GF represents a novel attractive candidate for preclinical evaluation.

Acknowledgment

This work was supported by a grant from the Toyama Support Center for Young Principal Investigators in Advanced Life Sciences, Japan, and a Grant in Aid for Scientific Research (No 24510314) from the Japan Society for the Promotion of Science.

Disclosure

The authors report no conflict of interest in this work.

References

1. Asuthkar S, Rao JS, Gondi CS. Drugs in preclinical and early-stage clinical development for pancreatic cancer. *Expert Opin Investig Drugs*. 2012;21:143–152.
2. The Editorial Board of the Cancer Statistics in Japan. *Cancer Statistics in Japan 2012*. Tokyo, Japan: Foundation for Promotion Cancer Research; 2012.
3. Hidalgo M. Pancreatic cancer. *N Engl J Med*. 2010;362:1605–1617.
4. Jemal A, Bray F, Center MM, Ferlay J, Ward E, Forman D. Global cancer statistics. *CA Cancer J Clin*. 2011;61:69–90.
5. Lionetto R, Pugliese V, Bruzzi P, Rosso R. No standard treatment is available for advanced pancreatic cancer. *Eur J Cancer*. 1995;31:882–887.
6. Philip PA, Benedetti J, Corless CL, et al. Phase III study comparing gemcitabine plus cetuximab versus gemcitabine in patients with advanced pancreatic adenocarcinoma: Southwest oncology group-directed intergroup trial S0205. *J Clin Oncol*. 2010;28:3605–3610.
7. Arumugam T, Ramachandran V, Fournier KF, et al. Epithelial to mesenchymal transition contributes to drug resistance in pancreatic cancer. *Cancer Res*. 2009;69:5820–5828.
8. Qiu MT, Ding XX, Hu JW, Tian HY, Yin R, Xu L. Fixed-dose rate infusion and standard rate infusion of gemcitabine in patients with advanced non-small-cell lung cancer: a meta-analysis of six trials. *Cancer Chemother Pharmacol*. 2012;70:861–873.
9. Conroy T, Desseigne F, Ychou M, et al. FOLFIRINOX versus gemcitabine for metastatic pancreatic cancer. *N Engl J Med*. 2011;364:1817–1825.
10. Von Hoff DD, Ramanathan RK, Borad MJ, et al. Gemcitabine plus nab-paclitaxel is an active regimen in patients with advanced pancreatic cancer: a phase I/II trial. *J Clin Oncol*. 2011;29:4548–4554.
11. Ko AH, Venook AP, Bergsland EK, et al. A Phase II study of bevacizumab plus erlotinib for gemcitabine-refractory metastatic pancreatic cancer. *Cancer Chemother Pharmacol*. 2010;66:1051–1057.
12. Sakamoto H, Kitano M, Suetomi Y, Maekawa K, Takeyama Y, Kudo M. Utility of contrast-enhanced endoscopic ultrasonography for diagnosis of small pancreatic carcinomas. *Ultrasound Med Biol*. 2008;34:525–532.
13. Feig C, Gopinathan A, Neesse A, Chan DS, Cook N, Tuveson DA. The pancreas cancer microenvironment. *Clin Cancer Res*. 2012;18:4266–4276.
14. Izuishi K, Kato K, Ogura T, Kinoshita T, Esumi H. Remarkable tolerance of tumor cells to nutrient deprivation: possible new biochemical target for cancer therapy. *Cancer Res*. 2000;60:6201–6207.
15. Awale S, Lu J, Kalauni SK, et al. Identification of arctigenin as an antitumor agent having the ability to eliminate the tolerance of cancer cells to nutrient starvation. *Cancer Res*. 2006;66:1751–1757.
16. Awale S, Nakashima EMN, Kalauni SK, et al. Angelmarin, a novel anti-cancer agent able to eliminate the tolerance of cancer cells to nutrient starvation. *Bioorg Med Chem Lett*. 2006;16:581–583.
17. Win NN, Awale S, Esumi H, Tezuka Y, Kadota S. Novel anticancer agents, kayeassamins A and B from the flower of *Kayea assamica* of Myanmar. *Bioorg Med Chem Lett*. 2008;18:4688–4691.
18. Win NN, Awale S, Esumi H, Tezuka Y, Kadota S. Novel anticancer agents, kayeassamins C–I from the flower of *Kayea assamica* of Myanmar. *Bioorg Med Chem*. 2008;16:8653–8660.
19. Win NN, Awale S, Esumi H, Tezuka Y, Kadota S. Bioactive secondary metabolites from *Boesenbergia pandurata* of Myanmar and their preferential cytotoxicity against human pancreatic cancer PANC-1 cell line in nutrient-deprived medium. *J Nat Prod*. 2007;70:1582–1587.
20. Win NN, Awale S, Esumi H, Tezuka Y, Kadota S. Panduratins D–I, novel secondary metabolites from rhizomes of *Boesenbergia pandurata*. *Chem Pharm Bull*. 2008;56:491–496.
21. Awale S, Linn TZ, Than MM, Swe T, Saiki I, Kadota S. The healing art of traditional medicines in Myanmar. *J Trad Med*. 2006;23:47–68.
22. Awale S, Ueda J, Athikomkulchai S, et al. Antiausterity agents from *Uvaria dac* and their preferential cytotoxic activity against human pancreatic cancer cell lines in a nutrient-deprived condition. *J Nat Prod*. 2012;75:1177–1183.
23. Guertin DA, Sabatini DM. Defining the role of mTOR in cancer. *Cancer Cell*. 2007;12:9–22.
24. Conroy T, Gavoille C, Samalin E, Ychou M, Ducreux M. The role of the FOLFIRINOX regimen for advanced pancreatic cancer. *Curr Oncol Rep*. 2013;15:182–189.
25. Saif MW. Advancements in the management of pancreatic cancer: 2013. *JOP*. 2013;14:112–118.
26. Schönthal AH. Endoplasmic reticulum stress and autophagy as targets for cancer therapy. *Cancer Lett*. 2009;275:163–169.
27. Schönthal AH. Gliomas: Aggravating endoplasmic reticulum stress by combined application of bortezomib and celexoib as a novel therapeutic strategy for glioblastoma. In: Hayat MA, editor. *Tumors of the Central Nervous System*. Dordrecht, The Netherlands: Springer; 2011;1.
28. Yang ZJ, Chee CE, Huang S, Sinicrope FA. The role of autophagy in cancer: therapeutic implications. *Mol Cancer Ther*. 2011;10:1533–1541.
29. Sato K, Tsuchihara K, Fujii S, et al. Autophagy is activated in colorectal cancer cells and contributes to the tolerance to nutrient deprivation. *Cancer Res*. 2007;67:9677–9684.
30. Choi KS. Autophagy and cancer. *Exp Mol Med*. 2012;44:109–120.
31. Gozuacik D, Kimchi A. Autophagy as a cell death and tumor suppressor mechanism. *Oncogene*. 2004;23:2891–2906.
32. Esumi H, Lu J, Kurashima Y, Hanaoka T. Antitumor activity of pyrvinium pamoate, 6-(dimethylamino)-2-[2-(2,5-dimethyl-1-phenyl-1*H*-pyrrol-3-yl)ethenyl]-1-methyl-quinolinium pamoate salt, showing preferential cytotoxicity during glucose starvation. *Cancer Sci*. 2004;95: 685–690.
33. Lu J, Kunimoto S, Yamazaki Y, Kaminishi M, Esumi H. Kigamicin D, a novel anticancer agent based on a new anti-austerity strategy targeting cancer cells' tolerance to nutrient starvation. *Cancer Sci*. 2004;95: 547–552.
34. Yardley DA. Combining mTOR inhibitors with chemotherapy and other targeted therapies in advanced breast cancer: rationale, clinical experience, and future directions. *Breast Cancer Basic Res Treat*. 2013;7:7–22.

Cancer Science
The official journal of the Japanese Cancer Association JCA

Identification of a lung adenocarcinoma cell line with CCDC6-RET fusion gene and the effect of RET inhibitors *in vitro* and *in vivo*

Makito Suzuki,[1,2,11] Hideki Makinoshima,[1,11] Shingo Matsumoto,[1,3] Ayako Suzuki,[4] Sachiyo Mimaki,[1] Koutatsu Matsushima,[1,2] Kiyotaka Yoh,[3] Koichi Goto,[3] Yutaka Suzuki,[4] Genichiro Ishii,[5] Atsushi Ochiai,[5] Koji Tsuta,[6] Tatsuhiro Shibata,[7] Takashi Kohno,[8] Hiroyasu Esumi[9] and Katsuya Tsuchihara[1,2,10]

[1]Division of Translational Research, Research Center for Innovative Oncology, National Cancer Center Hospital East, Kashiwa, Chiba; [2]Department of Integrated Biosciences, Graduate School of Frontier Sciences, The University of Tokyo, Kashiwa, Chiba; [3]Division of Thoracic Oncology, National Cancer Center Hospital East, Kashiwa, Chiba; [4]Department of Medical Genome Sciences, Graduate School of Frontier Sciences, The University of Tokyo, Kashiwa, Chiba; [5]Division of Pathology, Research Center for Innovative Oncology, National Cancer Center Hospital East, Kashiwa, Chiba; [6]Division of Pathology and Clinical Laboratories, National Cancer Center Hospital, Tokyo; Divisions of [7]Cancer Genomics; [8]Genome Biology, National Cancer Center Research Institute, Tokyo; [9]National Cancer Center Hospital East, Kashiwa, Chiba, Japan

(Received December 4, 2012/Revised April 1, 2013/Accepted April 1, 2013/Accepted manuscript online April 11, 2013/Article first published online May 12, 2013)

Rearrangements of the proto-oncogene *RET* are newly identified potential driver mutations in lung adenocarcinoma (LAD). However, the absence of cell lines harboring *RET* fusion genes has hampered the investigation of the biological relevance of RET and the development of RET-targeted therapy. Thus, we aimed to identify a *RET* fusion positive LAD cell line. Eleven LAD cell lines were screened for *RET* fusion transcripts by reverse transcription-polymerase chain reaction. The biological relevance of the *CCDC6-RET* gene products was assessed by cell growth, survival and phosphorylation of ERK1/2 and AKT with or without the suppression of RET expression using RNA interference. The efficacy of RET inhibitors was evaluated *in vitro* using a culture system and in an *in vivo* xenograft model. Expression of the *CCDC6-RET* fusion gene in LC-2/ad cells was demonstrated by the mRNA and protein levels, and the genomic break-point was confirmed by genomic DNA sequencing. Mutations in *KRAS* and *EGFR* were not observed in the LC-2/ad cells. CCDC6-RET was constitutively active, and the introduction of a siRNA targeting the *RET 3'* region decreased cell proliferation by downregulating RET and ERK1/2 phosphorylation. Moreover, treatment with RET-inhibitors, including vandetanib, reduced cell viability, which was accompanied by the downregulation of the AKT and ERK1/2 signaling pathways. Vandetanib exhibited anti-tumor effects in the xenograft model. Endogenously expressing CCDC6-RET contributed to cell growth. The inhibition of kinase activity could be an effective treatment strategy for LAD. LC-2/ad is a useful model for developing fusion RET-targeted therapy. (*Cancer Sci* 2013; 104: 896–903)

Lung cancer is the most common cause of cancer death worldwide.[1] The identification of oncogenic driver genes is to select the increasing number of small molecule inhibitors targeting these gene products.[2,3] In particular, in lung adenocarcinoma (LAD), the most dominant histological subtype of lung cancer, the application of kinase inhibitors for cases with specific gene alterations has been successful, that is, gefitinib and erlotinib for *EGFR* mutation-positive cases and crizotinib for *ALK* fusion-positive cases.[4–7] Furthermore, accumulating evidence has demonstrated somatic mutations and rearrangements of potential oncogenes, including *BRAF, ERBB2* and *ROS1*, in LAD.[8–10]

RET is one of the newest LAD driver genes.[11–15] *RET* gene is located on chromosome 10 and encodes a receptor tyrosine kinase,[16,17] and the oncogenic potential of this gene product has been suggested in several tumors, including thyroid cancer.[18–20] Recently, five independent groups identified aberrant fusion genes, *KIF5B-RET* and *CCDC6-RET* in clinical samples of LAD.[11–15] Ectopically expressed RET fusion products afforded NIH3T3 cells with anchorage-independent growth and tumorigenicity in nude mice.[11,14] Furthermore, KIF5B-RET-expressing H1299 cells exhibited growth factor-independent growth.[11] These findings strongly suggest the oncogenic activity of RET fusion products and also suggest the potential therapeutic efficacy of multi-kinase inhibitor targeting of RET using the abovementioned cells. However, LAD-derived cell lines harboring *RET* fusion genes had not been identified. Recently, Matsubara *et al.*[21] screened LAD cell lines that were sensitive to a RET inhibitor vandetanib and found a *CCDC6-RET* fusion gene-harboring cell line, LC-2/ad.

We have independently screened cell lines established from Japanese LAD samples by RT-PCR and found that LC-2/ad cells expressed the *CCDC6-RET* fusion gene product. We further examined whether LC-2/ad cells depend on RET fusion-mediated signaling. In addition, the antitumor effect of RET inhibitors in LC-2/ad cells was evaluated *in vitro* and *in vivo*.

Materials and Methods

Complete materials and methods were described in the supplementary information (Data S1. Materials and Methods).

Purchased materials. Cell lines were purchased from RIKEN Bio Resource Center, the Immuno-Biological Laboratories (Fujioka, Japan) and American Type Culture Collection. Procedures for western blotting was previously described.[22] Primary antibodies specific for RET and phospho-RET Tyr-905 were purchased from Epitomics (Burlingame, CA, USA) and Cell Signaling Technologies (Danvers, MA, USA), respectively. RET-targeting siRNA was purchased from Life Technologies (Carlsbad, CA, USA). Gefitinib, sunitinib malate and sorafenib were purchased from Santa Cruz Biotechnology (Dallas, TX, USA), Sigma-Aldrich (St. Louis, MO, USA) and Toronto Research Chemicals (Toronto, ON, Canada),

[10]To whom correspondence should be addressed.
E-mail: ktsuchih@east.ncc.go.jp
[11]These authors contributed equally to this work.

doi: 10.1111/cas.12175

respectively. Vandetanib, AZD6244 and BEZ235 were purchased from Selleck (Houston, TX, USA).

Multiplex RT-PCR. Reported *KIF5B/CCDC6-RET* fusion variants were detected by multiplex RT-PCR according to the procedures described elsewhere.[11,14]

Genomic DNA sequencing. LC-2/ad DNA was captured with custom hybridization probes targeting *CCDC6* intron 1 and *RET* whole gene (Agilent) followed by parallel sequencing on the MiSeq system (Illumina).

Real-time RT-PCR. Procedures for real-time RT-PCR was previously described.[22] The PCR primers used in the present study are shown in Table S1.

***In vivo* studies.** LC2/ad cells at 5.0×10^6 were subcutaneously inoculated to 8-week-old athymic nude mice (Clea Japan).[23] Vandetanib was administered once daily as a homogeneous suspension by oral gavage at a dosage of 50 mg/kg body weight.[24] The tumor volume was calculated as the product of a scaling factor ($\pi/6$) and the tumor length, width and height.[22] The study was approved by the Institutional Ethics Review Committee for animal experiments at the National Cancer Center.

Immunohistochemical analysis. The procedure for hematoxylin eosin staining and immunohistochemical (IHC) was previously described.[22,25]

Microarray analysis. Background information of clinical samples was described in a previous report.[26] The study was approved by the Institutional Review Boards of the National Cancer Center. Total RNA was analyzed using Affymetrix (Santa Clara, CA, USA) U133Plus2.0 arrays. The data were processed by the MAS5 algorithm, and the mean expression level of a total of 54 675 probes was adjusted to 1000 for each sample.

Results

Identification of the *CCDC6-RET* fusion gene in a Japanese LAD cell line. To identify *RET* fusion-derived mRNA expression in human LAD cell lines, all reported *KIF5B-RET* and *CCDC6-RET* gene products were screened by multiplex RT-PCR in 11 cell lines derived from Japanese patients. LC-2/ad cells were found to express *CCDC6-RET* mRNA at significantly higher levels, whereas the other cell lines did not exhibit any fusion gene products (Fig. 1a). The expressed fusion *RET* product was sequenced, and an in-frame fusion of *CCDC6* exon 1 and *RET* exon 12, which was identical to the previously reported *CCDC6-RET* fusion products, was identified (Fig. 1b).[14] We then identified a breakpoint of chromosome 10 by retrieving genomic DNA fragments, including the entire *RET* gene and intron 1 of *CCDC6*, by target capture system followed by parallel sequencing. The identified break-point between *CCDC6* intron 1 and *RET* exon 11 was confirmed by Sanger sequencing (Fig. 1b). Quantitative RT-PCR revealed that the expression of 3′ end of *RET* was increased comparable to that of *CCDC6*, whereas the transcript level of the 5′ end of *RET* was significantly lower (Fig. 1c). Consistent with the amount of transcript, western blotting using an antibody recognizing the C-terminus of RET isoform 2 detected a 60-kDa specific band equivalent to

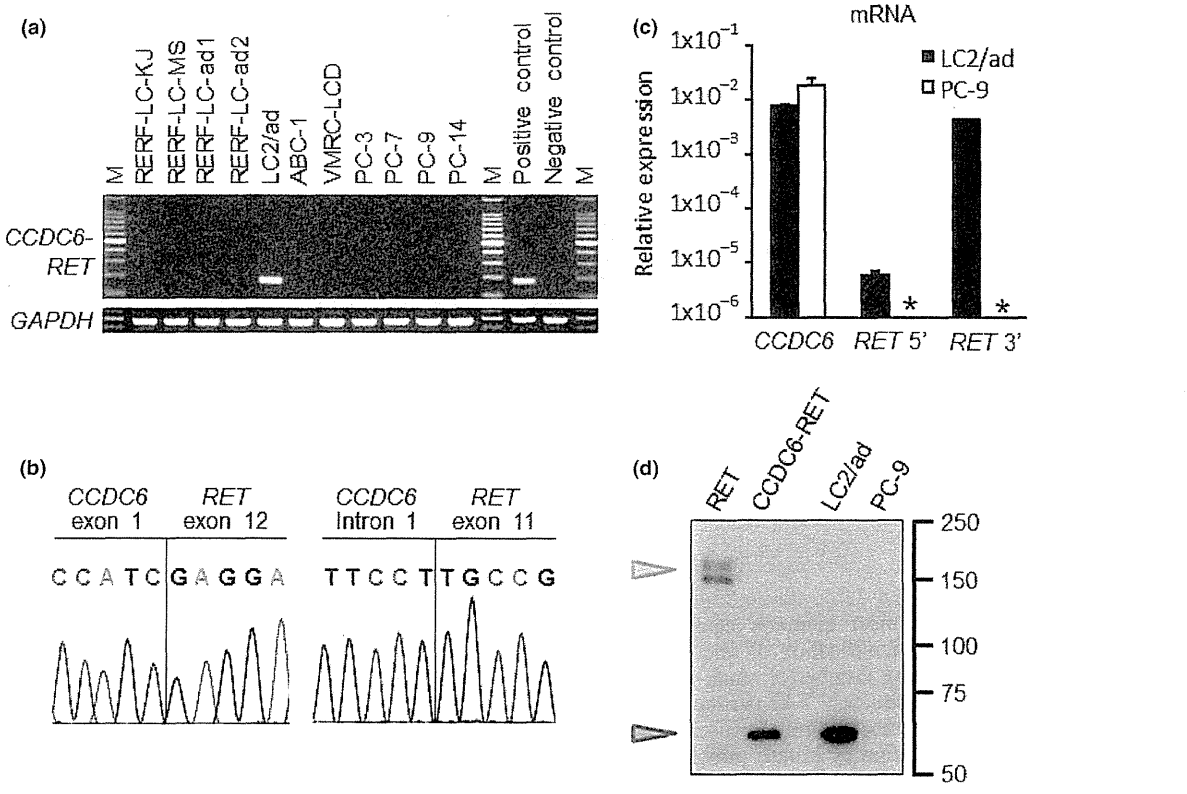

Fig. 1. Identification of the *CCDC6-RET* fusion gene. (a) Detection of *RET* fusion transcripts in lung adenocarcinoma (LAD) cell lines by multiplex reverse transcription-polymerase chain reaction (RT-PCR). (b) Sanger sequencing around the fusion point of the cDNA (left) and the breakpoint of the genomic DNA (right) of *CCDC6-RET* in LC-2/ad cells. (c) 3′ region-specific expression of *RET* mRNA in LC-2/ad cells. The 5′ or 3′ region of *RET* and *CCDC6* cDNA level was normalized to glyceraldehyde 3-phosphate dehydrogenase (*GAPDH*) expression. The data are shown as the mean ± standard deviation (SD) ($n = 3$). Asterisks indicate that mRNA expression were below the level of detection. (d) Specific expression of the CCDC6-RET fusion protein. Whole-cell lysates of LC2/ad and PC-9 cells and HEK293 cells transfected with wild-type RET (RET) or CCDC6-RET expression plasmids were subjected to western blot analysis to detect RET protein isoform 2. The LC-2/ad cells showed an approximately 60-kDa (red arrowhead) but not 170-kDa (blue arrowhead) band.

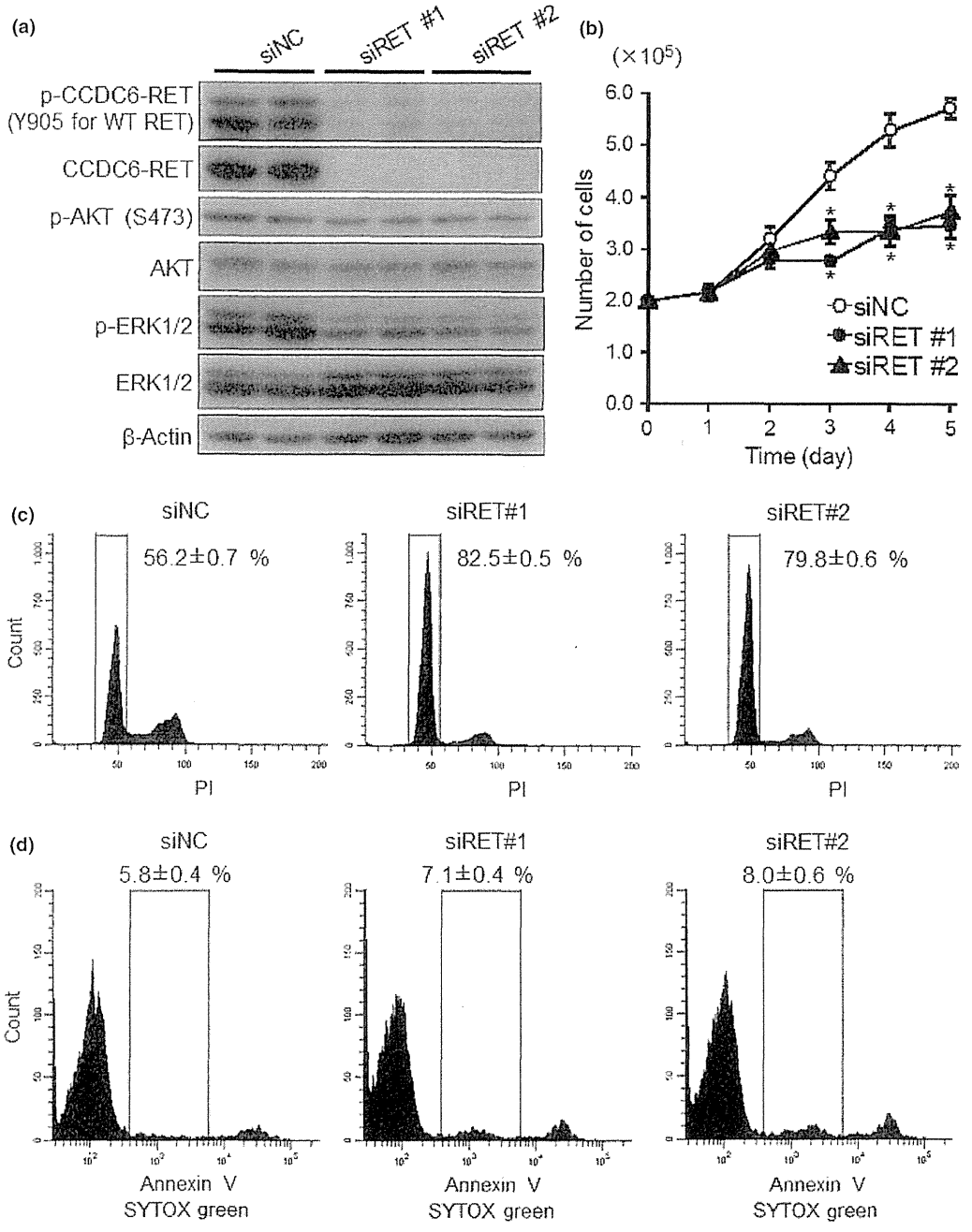

Fig. 2. Suppression of CCDC-RET expression by siRNA in LC-2/ad cells. (a) Western blot analysis of siRET-treated LC-2/ad cells. The siRNA transfected cell lysates were applied to the western blotting. (b) Involvement of RET suppression in cell growth inhibition. LC-2/ad cells transfected with siRNAs were incubated for the indicated times. The data are shown as the mean ± standard deviation (SD) (n = 4). *P < 0.01 (Student's t-test). (c,d) The DNA ploidy (c) and Annexin V-positive population (d) of siRET-transfected LC-2/ad cells. After 72 h of siRNA transfection, the cells were subjected to DNA ploidy analysis and Annexin V staining. The data are shown as the mean ± SD (n = 4).

the estimated size of the fusion protein composed of 503 amino acids (GeneBank BAM36435), whereas no significant signal was detected that approximated the size of wild-type RET, 170-kDa (Fig. 1d).[11] Taken together, we concluded that LC-2/ad cells express *CCDC6-RET* fusion gene products. *KRAS* exon 2 and *EGFR* exon 19 and 21 were examined by Sanger sequencing, but no obvious mutation was confirmed (Fig. S1).

CCDC6-RET-dependent ERK1/2 phosphorylation and the proliferation of LC-2/ad cells. We suppressed *RET* expression by RNAi to characterize the function of CCDC6-RET in LC-2/ad cells. For avoiding off-target siRNA effects, two different sequences of siRNA directed against the 3′ region of *RET* (siRET#1 and #2) and a nontargeting siRNA (siNC) were used. When compared to siNC, a significant reduction in mRNA expression was observed by quantitative RT-PCR detecting the 3′ end of the *RET* mRNA: 66.5% for siRET#1 and 94.2% for siRET#2 (Fig. S2). Western blot analyses also revealed significant decreases in the expression of CCDC6-RET protein (60-kDa) upon the introduction of siRET#1 and #2 compared to the control siNC in the LC-2/ad cells

doi: 10.1111/cas.12175